DEVELOPMENTS IN PALEOENVIRONMENTAL RESEARCH

DENDROCLIMATOLOGY

Progress and Prospects

Volume 11

Edited by
Malcolm K. Hughes, Thomas W. Swetnam and
Henry F. Diaz

Springer

Dendroclimatology

Progress and Prospects

Edited by

Malcolm K. Hughes

University of Arizona, Tucson, AZ, USA

Thomas W. Swetnam

University of Arizona, Tucson, AZ, USA

Henry F. Diaz

University of Colorado, Boulder, CO, USA

Springer

Part III
Reconstruction of Climate Patterns and Values Relative to Today's Climate

Chapter 7
Dendroclimatology from Regional to Continental Scales: Understanding Regional Processes to Reconstruct Large-Scale Climatic Variations Across the Western Americas

Ricardo Villalba, Brian H. Luckman, Jose Boninsegna, Rosanne D. D'Arrigo, Antonio Lara, Jose Villanueva-Diaz, Mariano Masiokas, Jaime Argollo, Claudia Soliz, Carlos LeQuesne, David W. Stahle, Fidel Roig, Juan Carlos Aravena, Malcolm K. Hughes, Gregory Wiles, Gordon Jacoby, Peter Hartsough, Robert J.S. Wilson, Emma Watson, Edward R. Cook, Julian Cerano-Paredes, Matthew Therrell, Malcolm Cleaveland, Mariano S. Morales, Nicholas E. Graham, Jorge Moya, Jeanette Pacajes, Guillermina Massacchesi, Franco Biondi, Rocio Urrutia, and Guillermo Martinez Pastur

Abstract Common patterns of climatic variability across the Western Americas are modulated by tropical and extra-tropical oscillatory modes operating at different temporal scales. Interannual climatic variations in the tropics and subtropics of the Western Americas are largely regulated by El Niño-Southern Oscillation (ENSO), whereas decadal-scale variations are induced by long-term Pacific modes of climate variability such as the Pacific Decadal Oscillation (PDO). At higher latitudes, climate variations are dominated by oscillations in the Annular Modes (the Arctic and Antarctic Oscillations) which show both interannual and longer-scale temporal oscillations. Here we use a recently-developed network of tree-ring chronologies to document past climatic variations along the length of the Western Cordilleras. The local and regional characterization of the relationships between climate and tree-growth provide the basis to compare climatic variations in temperature- and precipitation-sensitive records in the Western Americas over the past 3–4 centuries. Upper-elevation records from tree-ring sites in the Gulf of Alaska and Patagonia reveal the occurrence of concurrent decade-scale oscillations in temperature during the last 400 years modulated by PDO. The most recent fluctuation from the cold- to the warm-phase of the PDO in the mid 1970s induced marked changes in

R. Villalba (✉)
Departamento de Dendrocronología e Historia Ambiental, Instituto Argentino de Nivología, Glaciología y Ciencias Ambientales (IANIGLA), CONICET, CC 330, 5500, Mendoza, Argentina
e-mail: ricardo@mendoza-conicet.gob.ar

M.K. Hughes et al. (eds.), *Dendroclimatology*, Developments in Paleoenvironmental Research 11, DOI 10.1007/978-1-4020-5725-0_7,

tree growth in most extratropical temperature-sensitive chronologies in the Western Cordilleras of both Hemispheres. Common patterns of interannual variations in tree-ring chronologies from the relatively-dry subtropics in western North and South America are largely modulated by ENSO. We used an independent reconstruction of Niño-3 sea surface temperature (SST) to document relationships to tree growth in the southwestern US, the Bolivian Altiplano and Central Chile and also to show strong correlations between these regions. These results further document the strong influence of SSTs in the tropical Pacific as a common forcing of precipitation variations in the subtropical Western America during the past 3–4 centuries. Common patterns of interdecadal or longer-scale variability in tree-ring chronologies from the subarctic and subantarctic regions also suggest common forcings for the annular modes of high-latitude climate variability. A clear separation of the relative influence of tropical versus high-latitude modes of variability is currently difficult to establish: discriminating between tropical and extra-tropical influences on tree growth still remains elusive, particularly in subtropical and temperate regions along our transect. We still need independent reconstructions of tropical and polar modes of climate variability to gain insight into past forcing interactions and the combined effect on climates of the Western Americas. Finally, we also include a series of brief examples (as ‘boxes’) illustrating some of the major regional developments in dendrochronology over this global transect in the last 10 years.

Keywords Dendrochronology · Regional scale · Continental scale · Climate variations · Americas

7.1 Introduction

Instrumental records show that the climate system is characterized by low- and high-latitude patterns or modes of variability such as the El Niño/Southern Oscillation (ENSO) in the equatorial Pacific and the Arctic (AO) and Antarctic (AAO) Oscillations in the extratropics. The Pacific and high-latitude atmospheric circulation features associated with interannual to decadal variability of climate over the Americas exhibit large spatial and temporal variance that remains poorly documented. The resulting regional climate variability has enormous socioeconomic impacts, as was vividly demonstrated by the disastrous flooding in Paraguay and eastern Argentina, and the extended drought and massive wildfires in the southwestern United States and Mexico during the 1997–1998 El Niño event. At decadal scales, the prolonged shift in sea surface temperature (SST) patterns over the north and south Pacific Ocean after 1976 (Graham 1994) has resulted in ocean and atmospheric changes that have caused costly changes in commercial fish populations in the eastern north Pacific (Mantua and Hare 2002; Chavez et al. 2003; Beamish et al. 2004) and a greatly reduced carrying capacity for commercially important

Patagonian grasslands. These coherent interhemispheric changes in annual and decadal climate patterns associated with the Pacific Decadal Oscillation (PDO) appear to have been driven by fundamental changes in the hydrologic cycle of the tropical Pacific Ocean (Graham 1994; Evans et al. 2001a, b; Villalba et al. 2001).

Hemispheric-scale networks of instrumental and proxy climate data are needed to document and help understand these changes in the ocean-atmosphere system and their impact on the Americas.

Substantial recent effort has been devoted to the development of ocean-atmospheric monitoring arrays in the tropical Pacific (e.g., TOGA/TAO, TOPEX/POSEIDON; Wallace et al. 1998). The cost of these arrays has already been justified by the economic benefits provided by the long-lead climate forecasting associated with recent ENSO warm events. However, there is clear instrumental and paleoclimatic evidence that, for example, the frequency of warm and cold ENSO events has been subject to substantial changes over the past several centuries. The available instrumental meteorological records are simply too short to clearly define the important temporal and spatial modes inherent in the low-frequency dynamics of the Pacific and high-latitude major circulation systems. As these decade-scale changes in atmospheric circulation have strong impacts on regional climates and society, understanding these phenomena will improve the skill of long-range climate forecasting. There is increasing evidence (e.g., Gershunov and Barnett 1998) that they modulate the character of high-frequency ENSO teleconnections, producing more extreme and more predictable anomaly patterns when the two systems are in phase.

The Western America Cordilleras provide a contiguous latitudinal transect of mountainous terrain flanking the world's largest ocean that invites comparative studies of climate variations along the Americas. The American Cordilleras can provide high-quality proxy climate records over most of their lengths. Tree rings provide the most broadly distributed, annually resolved source of proxy climate data throughout the Cordillera and thereby supply the comprehensive baseline data necessary to evaluate natural climate variability on different temporal and spatial scales.

Progress in dendroclimatology across the Americas has been concerned with the geographical expansion of the research from the local to regional and continental scales. The work of Harold Fritts (1976, 1991) and co-workers in the 1970s represented the first attempt to reconstruct the patterns of spatial variation in temperature, precipitation, and atmospheric pressure across North America and the Pacific Ocean, based on 65 ring width chronologies from the western United States. Collaborative work between several research groups during the past 10 years (Meko et al. 1993; Cook et al. 1999, 2004) have extended this methodology by compiling 835 chronologies from Canada, the United States, and Mexico to reconstruct a gridded network of 297 summer Palmer Drought Severity Indices (PDSIs) across North America that spans the past 500–600 years (or longer) over much of the grid (Cook et al. 2004). Following these initiatives, new projects have continued to develop databases of tree-ring chronologies that cover large areas in the Western Americas (Fig. 7.1).

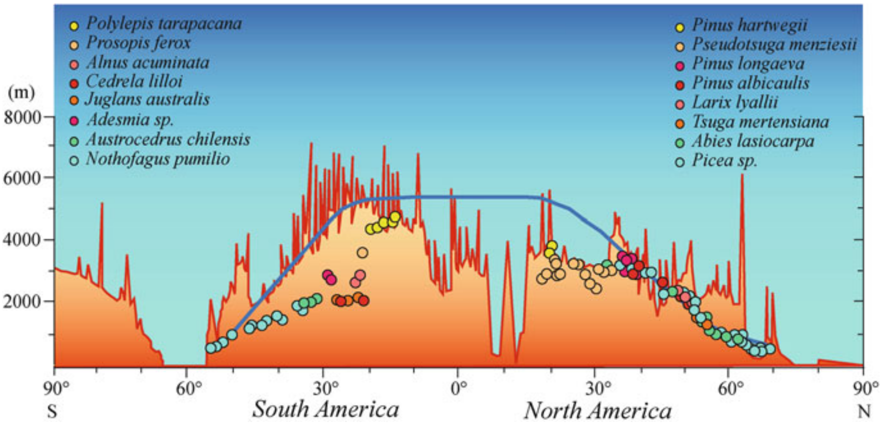

Fig. 7.1 Cross-section from the South to North Pole across the Western American Cordilleras showing changes in elevation with latitude, the approximate location of the mean annual zero degree (0°C) line, and the distribution of upper-elevation tree-ring chronologies. Major tree taxa used for developing the chronologies are also indicated

One of the Collaborative Research Networks supported by the Inter-American Institute for Global Change Research (IAI) was focused around the development of tree line chronologies from Alaska to Tierra del Fuego (Luckman and Boninsegna 2001). Using this research as a framework, we discuss in this chapter some of the most significant developments in tree-ring research across the western Americas, reviewing local- and regional-scale studies and how they contribute to our understanding of present and past variations in the circulation modes of climate variability at continental and interhemispheric scales. The Western Cordilleras of the Americas runs transverse to the generally latitudinal organization of the major climate-ocean circulation systems, and therefore past variations in the major modes of general circulation dynamics linked to El Niño/Southern Oscillation, Pacific Decadal Oscillation, the Arctic and Antarctic Oscillations can be investigated by using tree-ring records from this global-scale transect.

7.2 Oscillatory Modes of Climate Variability Across the Western Cordilleras

Instrumental records show that the climate system is characterized by low- and high-latitude patterns or modes of variability. These dominant modes of climate variability fluctuate at many different temporal scales. The best known is the El Niño-Southern Oscillation phenomenon in the tropical Pacific, which dominates global climate variations on interannual timescales, mostly ranging from 3 to 6 years (Wallace et al. 1998). On longer than interannual timescales, the dominant climate pattern in the Pacific Ocean has an ENSO-like spatial distribution of surface temperature and atmospheric circulation and has been identified as the Pacific

Decadal Oscillation in the extratropical north Pacific, the Pacific Interdecadal Mode in the whole Pacific basin, and as the Global Residual (GR) index on a global scale (Mantua et al. 1997; Garreaud and Battisti 1999; Enfield and Mestas-Nuñez 2000). Decadal variability in the climate of the Atlantic basin has also been identified (Deser and Blackmon 1993), but its interhemispheric climate effects on the Western Cordilleras are less well known.

The Arctic and Antarctic Oscillations are the dominant modes of climate variability at the highest latitudes in both hemispheres. The positive state of these annular modes is associated with intensified subtropical highs and strong polar lows, which drive a strong extratropical circulation. They also exhibit short- and long-term modes of variability.

7.2.1 El Niño/Southern Oscillation (ENSO)

Modern interannual variations in the Pacific basin and their interhemispheric effects on the Western Cordilleras have been extensively documented. The pattern of sea surface temperature associated with ENSO, measured as the SST anomalies from 6°N to 6°S, 180° to 90°W (the Cold Tongue [CT] index of Deser and Wallace 1990), are indicated by correlations mapped in Fig. 7.2. Positive correlations indicate regions where the ocean is warmer when the index is positive. As can be expected by the nature of the CT index, the strongest correlation with SST occurs in the tropical Pacific. The subtropical north and south Pacific Oceans are dominated by anomalies out of phase with the ones occurring in the tropical Pacific, forming a symmetric pattern about the equator.

The continental effects of the ENSO-related climate variations in terms of surface air temperature (SAT) and precipitation along the Western Cordilleras are remarkably symmetric about the equator (Fig. 7.3a,b). Positive temperatures in the tropical Pacific are associated with deeper than normal Aleutian lows, and the resulting steep north-south gradient in the middle latitudes brings storms and precipitation to the southwestern and southeastern parts of North America. In a rough parallel to the circulation changes in the Northern Hemisphere, the steeper gradient in pressure over the southeastern Pacific related to El Niño events, corresponds to deflections of the low-pressure systems and the associated storms towards the subtropical belt of South America, increasing precipitation in central Chile (Fig. 7.3b). Positive CT indices are associated with warmer than normal surface conditions all along the American Cordilleras (Fig. 7.3a). El Niño brings cool temperatures to the southeastern United States and to the eastern Amazon basin (Dettinger et al. 2001).

7.2.2 Pacific Interdecadal Mode

Using instrumental records, several studies have reported Pacific decadal-scale oscillatory modes (Trenberth and Hurrell 1994; Mantua et al. 1997; Zhang et al.

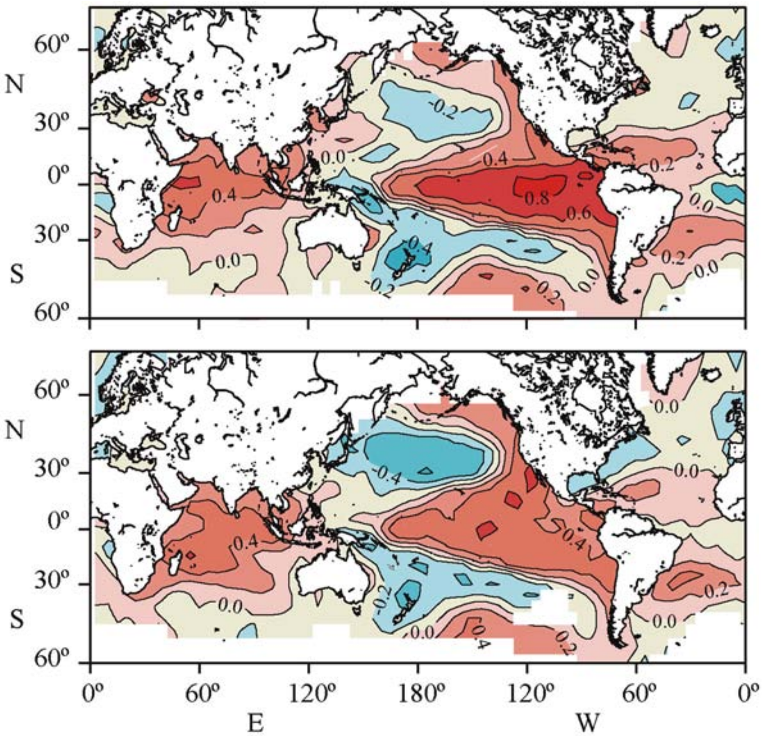

Fig. 7.2 Correlation coefficients between annual-averaged sea surface temperatures and (*upper*) Cold Tongue (CT) index (1903–1990) and (*lower*) Global Residual (GR) index (1903–1990). The contour interval is 0.2, *dashed* where negative. Correlations greater than +0.2, or less than –0.2, pass a two-tail Student's *t*-test of being different from zero at 95% significance levels (modified from Dettinger et al. 2001)

1997; Garreaud and Battisti 1999; Deser et al. 2004). The physical processes responsible for the decadal variability across the Pacific remain uncertain, but are connected to well-documented pan-Pacific changes in the atmosphere and ocean in recent decades. For example, the 1976–1977 climatic shift influenced climatic conditions all along the western Americas and is a remarkable manifestation of this Pacific decade-scale climatic variability (Ebbesmeyer et al. 1991). Sea surface temperatures along the equatorial belt and along the coast of the Americas become warmer, while further west at temperate latitudes the sea surface becomes cooler (Fig. 7.2). The array of atmospheric and oceanic changes that have been linked to these basin-wide regime shifts is collectively referred to as the Pacific Decadal Oscillation or the Pacific Interdecadal Mode (Mantua et al. 1997; Enfield and Mestas-Nuñez 2000). Warm and wet decades in the equatorial Pacific tend to be marked by extratropical circulation patterns that bring mild weather conditions to coastal Alaska and northern Patagonia. In contrast to the interannual mode of ENSO variability, the decadal mode is characterized by less pronounced anomalies in the

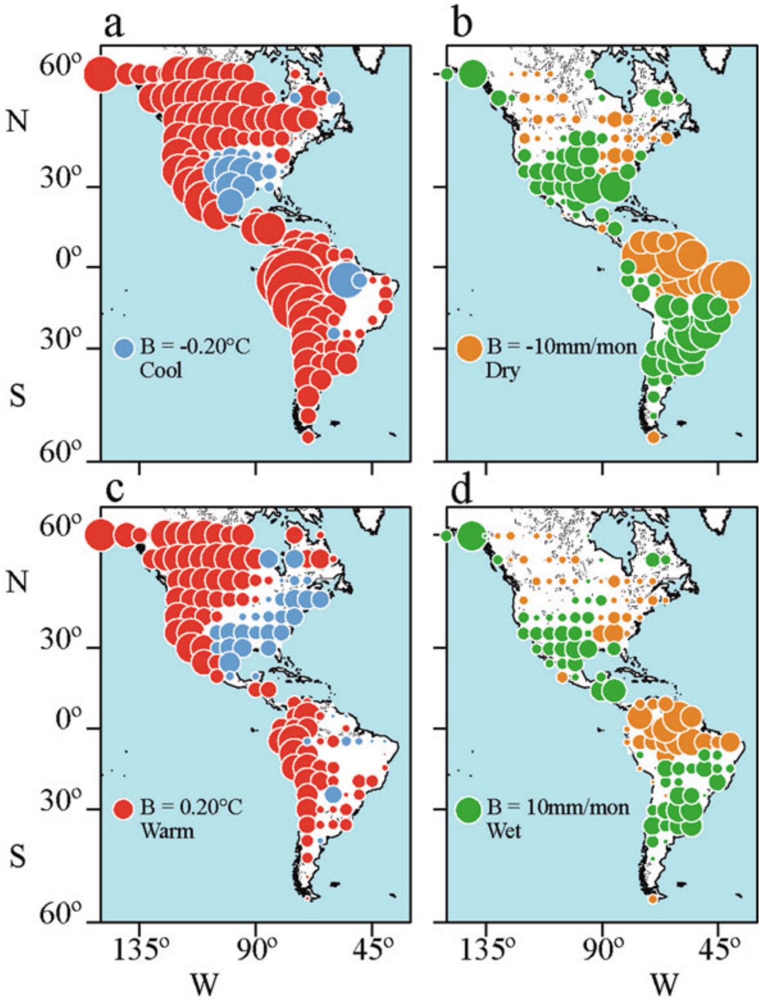

Fig. 7.3 Regression coefficients (B) estimated during the interval 1904–1990, relating Cold Tongue (CT) index to October–September (**a**) surface air temperatures, and (**b**) precipitation. Figures (**c**) and (**d**) are same as (**a**) and (**b**) but for the Global Residual (GR) index. Radii of circles are proportional to the magnitude of regression coefficients: *red* and *light blue*, respectively, for positive and negative relations with surface air temperatures; *green* and *light brown*, respectively, for positive and negative relations with precipitation. The *circles*, lower left in each diagram, indicate the scale of influences. Temperatures from an updated version of the monthly, $5^\circ \times 5^\circ$-gridded temperature anomaly set of Jones et al. (1986a, b), and land precipitation anomalies on a similar grid from Eischeid et al. (1991) were compared with CT and GR. Regression coefficients may be affected by the magnitude of the variable used in the analysis. The lack of significant regression coefficients between CT and precipitation in the central Andes along the South American Pacific coastline is likely due to the reduced precipitation across this region (modified from Dettinger et al. 2001)

eastern Pacific (the classic key ENSO region) and is not narrowly confined along the equator. The documented decadal oscillatory mode of Pacific SST shows anomalies in the western Pacific that extend to the northeast and southeast into the American subtropics.

Overall, the atmospheric expressions of the ENSO-like climate variations on both interannual and decadal timescales are remarkably symmetric about the equator, especially on the Pacific coast of western Americas (Fig. 7.3c,d). Positive variations in the CT and GR are associated with equatorward diversions of the westerlies, enhancement of the low-pressure systems, and storms from the midlatitude Pacific basin toward North and South America subtropical latitudes (Dettinger et al. 2001).

7.2.3 Annular Modes

The Northern Hemisphere (NAM) and Southern Hemisphere (SAM) Annular Modes dominate extratropical climate variability throughout their respective hemispheres (Thompson and Wallace 2000). The NAM is alternatively referred to as the North Atlantic Oscillation (NAO) (Hurrell and van Loon 1997) and the Arctic Oscillation (Thompson and Wallace 2000); whereas the SAM is alternatively referred to as the High-Latitude Mode (Karoly 1990) and the Antarctic Oscillation (Gong and Wang 1999; Thompson and Wallace 2000).The structures of the Northern Hemisphere and Southern Hemisphere Annular Modes are shown to be remarkably similar, not only in the zonally averaged geopotential height and zonal wind fields, but in the mean meridional circulations as well. Both annular modes are associated with equivalent barotropic vacillations in the strength of the zonal flow between centers of action located at ~35°–40° and ~55°–60° latitude. The SAM is moderately symmetric about the pole, but due to the more complex distribution of the northern continents, the NAM is more evident over the north Atlantic and the north Pacific Oceans (Fig. 7.4).

Periods when the zonal flow along ~55°–60° latitude is anomalously westerly (the so-called high-index polarity of the annular modes) are characterized by lower than normal geopotential heights and temperatures over the polar cap, and by higher than normal geopotential heights and temperatures in the middle latitudes centered at ~45°. As atmospheric variability in the Northern Hemisphere is largest in winter, the spatial pattern of the conventional NAM mostly reflects the winter variability (Thompson and Wallace 2000). The positive polarity of the winter AO is associated with positive surface air temperature anomalies throughout the high latitudes of Eurasia and much of North America, and negative anomalies over extreme eastern Canada, North Africa, and the Middle East. This zonally asymmetric pattern of SAT anomalies is evident throughout the year except during the Northern Hemisphere summer months (Thompson and Wallace 2000). The leading mode of the Empirical Orthogonal Function (EOF) in summer months has a smaller meridional scale than the conventional NAM. Associated summertime low-level temperature anomalies show more extended warm anomalies over the midlatitudes than the winter NAM

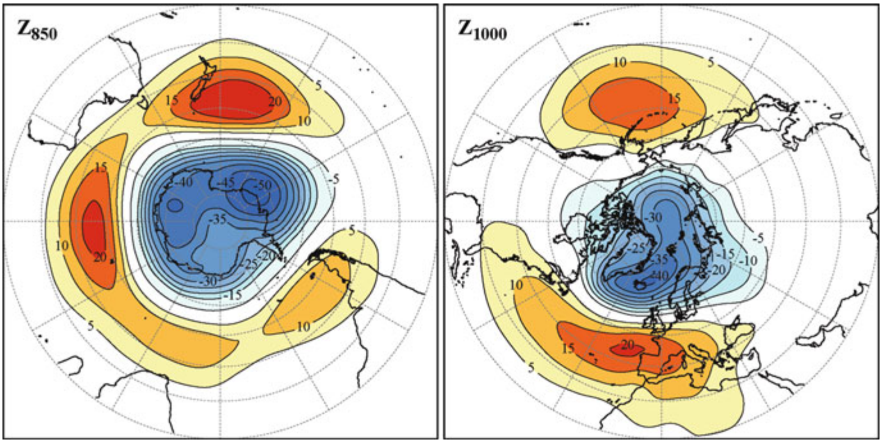

Fig. 7.4 High-latitude annular modes. The Southern Annular Mode (SAM) or Antarctic Oscillation (AAO) mode is moderately symmetric about the pole (*left*), but due to the more complex distribution of the northern continents, the Northern Annular Mode (NAM) or Arctic Oscillation (AO) is more evident over the North Atlantic and the north Pacific Oceans. Zonal-mean geopotential height fields are represented with contour intervals of 5 m (modified from Thompson and Wallace 2000)

counterpart, especially over Europe, the Sea of Okhotsk, and northern America. For example, the summer NAM pattern accounts for many of the anomalous weather features observed during the summer of 2003. Temperature anomalies over northwestern Eurasia, northeastern Siberia, and Canada during that period exceeded 3°C (Ogi et al. 2004).

The positive polarity of the Southern Hemisphere Annular Mode is associated with cold anomalies over most of Antarctica. The one notable exception is the Antarctic Peninsula and southern South America, where the enhanced westerlies related to the high SAM polarity increase the advection of relatively warm oceanic air over the lands (Thompson and Solomon 2002). The observed trend in the SAM toward stronger circumpolar flow is in the same sense as the trends that have dominated the Northern Hemisphere extratropical circulation over the past few decades. The occurrence of positive trends in both the NAM and SAM suggests that the trends reflect processes that transcend the high-latitude climate of a particular hemisphere.

7.3 Tree-Ring Records Across the Western Americas

A major result of the Collaborative Research Network has been the consolidation and expansion of tree-ring collections across the traditional research regions of North and South America, the focusing on key areas, and the start of many developments in new regions of Canada, Mexico, Peru, Bolivia, Chile, and Argentina (Boxes 7.1, 7.2, 7.3, 7.6 and 7.8). Along the western coasts of North and South

Box 7.1 Climate signals in Gulf of Alaska tree-ring records

A network of climatically sensitive tree-ring records has been compiled for the Gulf of Alaska (GOA) region, and the records have been used to develop time series of temperatures over the past one to two millennia (Box Fig. 7.1). This region is strongly sensitive to the climatic effects of the Pacific Decadal Oscillation (PDO), and the GOA chronologies show evidence for decadal-scale regime shifts, including the noteworthy 1976 transition in Pacific climate. These records have been linked to sea surface temperature (SST) variations in the Pacific and have been included in reconstructions of the PDO (e.g., D'Arrigo et al. 2001). On longer timescales, century to millennial temperature variations are evident and are linked to glacial changes in southern Alaska.

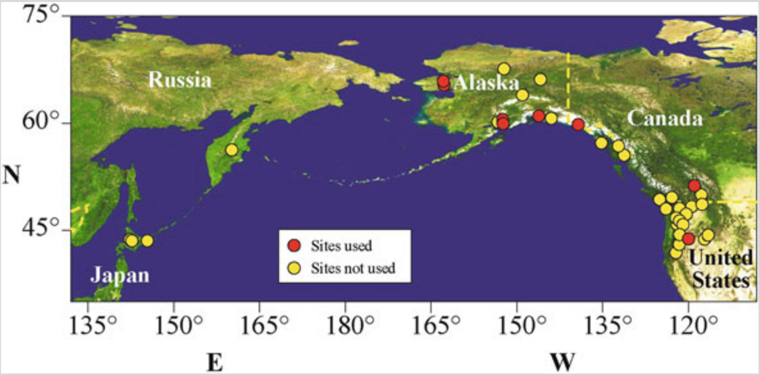

Box Fig. 7.1 Map of North Pacific region showing locations of tree-ring sites (*yellow*) used as candidate predictors of the tropical Indo-Pacific climate index (NPI). Sites in *red* are those included in the regression model used to reconstruct the NPI. Some dots represent more than one site (D'Arrigo et al. 2005)

Analyses of instrumental data demonstrate robust linkages between decadal-scale North Pacific and tropical Indo-Pacific climatic variability, yet information on the tropical–high-latitude climate connection is limited prior to the twentieth century. Gulf of Alaska and western Canadian tree-ring records were used to reconstruct the December–May North Pacific index (NPI—an index of the atmospheric circulation related to the Aleutian low-pressure cell) from 1600 to 1983 (D'Arrigo et al. 2005; Box Fig. 7.2). This NPI reconstruction shows evidence for the climatic regime shifts seen in the instrumental NPI data, and for additional events in prior centuries. It correlates significantly with both instrumental tropical climate indices and a coral-based reconstruction of an optimal tropical Indo-Pacific climate index (OTI), supporting evidence for a tropical/North Pacific link extending as far west as the western Indian Ocean. The coral-based reconstruction (1781–1993) shows the twentieth-century regime shifts evident in the instrumental NPI and OTI, as well as previous shifts. Changes in the strength of the correlation between the NPI and OTI reconstructions over time, and the timing of regime shifts in both series prior to the twentieth century, suggest a varying tropical influence on North Pacific climate, with greater influence in the twentieth century. One likely mechanism is the low-frequency variability of the El Niño/Southern Oscillation (ENSO) and its varying impact on Indo-Pacific climate.

—R. D'Arrigo, G. Wiles, and R. Wilson

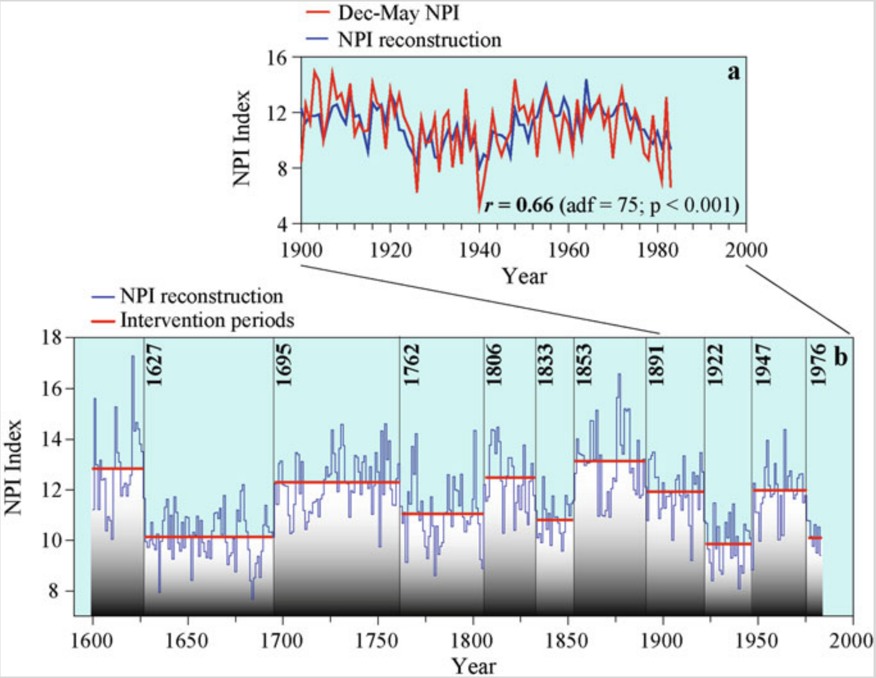

Box Fig. 7.2 Tree-ring-based reconstruction of the tropical Indo-Pacific climate index (NPI): (**a**) actual and estimated December–May NPI for the 1900–1983 calibration period, adf = adjusted degrees of freedom; (**b**) reconstruction of the December–May NPI from AD 1600 through 1983 based on North Pacific tree-ring data. The highlighted phase shifts were identified by using intervention analysis (significant at the 90% confidence level; D'Arrigo et al. 2005)

America, there is a gradual environmental gradient from the relatively dry-warm subtropics to the wet-cold high latitudes. Tree-ring records from subtropical regions, such as the southwestern United States and central Chile, are remarkably sensitive to precipitation variations (Boninsegna 1988; Cook et al. 2004; LeQuesne et al. 2006). In the transitional zones to higher latitudes, tree-ring responses to climate are largely determined by site conditions. Depending on elevation, aspect, slope, and soil characteristics, tree growth can be influenced by temperature, precipitation, or more commonly by a combination of both. In the extreme wet and cold environments at high-elevation or high-latitude upper tree lines, temperature is the major limiting factor controlling tree growth (Wiles et al. 1996; Luckman et al. 1997; Wiles et al. 1998; Aravena et al. 2002; Villalba et al. 2003; Lara et al. 2005). These changes in tree response with latitude were instrumental in setting the strategies for selecting tree-ring records sensitive to temperature and precipitation variations along the western Americas. Temperature reconstructions based on upper-elevation chronologies on mountains near the coasts around the Gulf of Alaska and northern Patagonia were selected as proxy records of temperature for North and South America, respectively. Tree-ring records from mesic to dry environments in the southern-central United States, the Bolivian Altiplano, and central Chile were used for the interhemispheric comparison of precipitation-sensitive records across the American Cordilleras (Fig. 7.1). The available data and maturity of dendroclimatological research differ considerably between regions, and therefore the kind of comparison between regional records and forcings will be different across the north-south transect.

7.3.1 Temperature-Sensitive Records

The strong cross-equatorial symmetries of SST, continental temperature, and continental precipitation patterns documented from instrumental records motivated the search in high-resolution proxy records for common spatial patterns of climate variability across the western Americas during the past centuries. Have the patterns of climate variability documented during the instrumental period been recurrent in previous centuries? Were these patterns different during the dominantly cooler conditions during the first half of the nineteenth century? Answers to these questions can provide useful information on the stationary nature of climate variations and how they could change under different global atmospheric conditions.

Box 7.2 Studies from the Canadian Cordillera

During the last 5 years, significant progress has been made in dendrochronological and dendroclimatic studies in the Canadian Cordillera (49°–65°N), building on limited earlier collections. Sampling has targeted temperature-sensitive sites at altitudinal tree line (*Picea engelmanni*, *P. glauca*, *Larix lyallii*, *Pinus albicaulis*, and *Abies lasiocarpa*) and moisture-sensitive sites at the lower forest border (*Pseudotsuga menziesii* and *Pinus ponderosa*), mainly using a network approach to isolate regional rather than local signals. Although initially focused on the southern Cordillera (ca. 125 chronologies), over 100 new sites have been sampled in the Yukon over the last 5 years. Studies at tree line in the Coast Ranges of British Columbia and Vancouver Island have developed several single- and multiple-species chronology networks (*Tsuga mertensiana*, *T. heterophylla*, and *Chamaecyparis nootkatensis*) that include sites with the potential for millennial-length reconstructions (see http://geog.uvic.ca/dept/uvtrl/uvtrl.htm). In the southern Cordillera, the network of low-elevation, moisture-sensitive sites has been used to reconstruct spatial patterns of precipitation and drought over the last three to four centuries (Watson and Luckman 2004a, 2005), and these data have been incorporated into the new gridded Palmer Drought Severity Index (PDSI) network developed by Cook et al. (2004).

New ring width and density data have been used to revise and extend a millennial-length (950–1994) summer temperature record from the Canadian Rockies (Box Fig. 7.3). Comparison with adjacent areas (e.g., Wiles et al. 2004) and global Northern Hemisphere curves suggests this is a regionally representative record. The influence of Pacific-forced decadal-scale variability in this record is more subtle, but the low-frequency signal suggests solar forcing has been an important control of summer temperature patterns in this region.

The use of multispecies networks allows the combination of temperature- and/or precipitation-sensitive chronologies to investigate climate-related phenomena that are influenced by the combined variation of temperature and precipitation. Box Figure 7.4 shows a reconstruction of glacier mass balance using independent tree-ring-derived summer and winter balances. Although winter balance (precipitation input) is strongly controlled by atmospheric circulation patterns from the Pacific, summer balance (mass loss through melt) is driven primarily by solar radiation. The major periods of positive net balance reflect a combination of higher winter inputs and cooler summers rather than summer temperatures alone. Future work can adopt similar approaches to the reconstruction of streamflow and other climate-related variables.

—B.H. Luckman, R.J.S. Wilson, and E. Watson

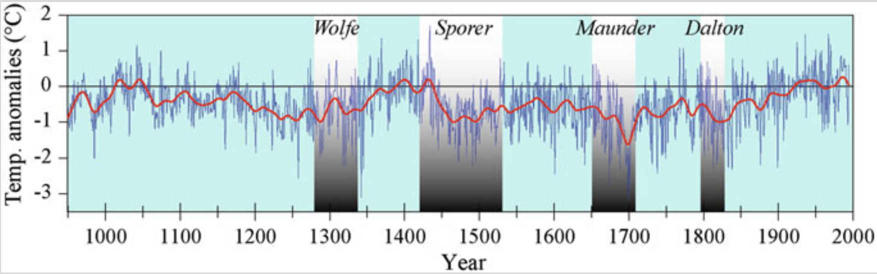

Box Fig. 7.3 Maximum May–August temperatures at the Columbia Icefield, Canadian Rockies. Temperatures are anomalies based on 1901–1980 means smoothed with a 30-year filter. Vertical bars represent significant sunspot minima (Luckman and Wilson 2005)

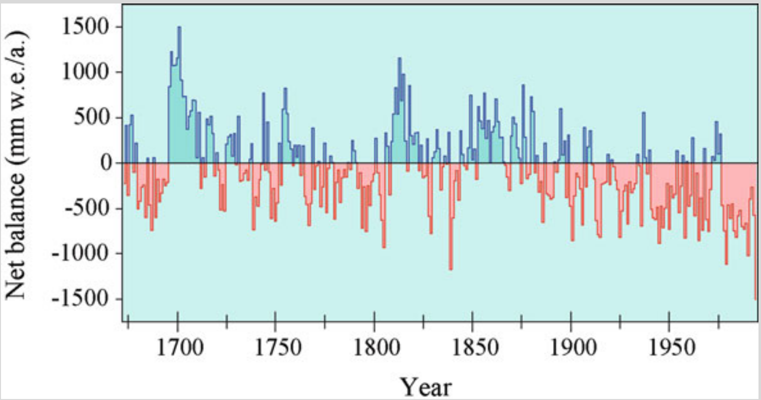

Box Fig. 7.4 Reconstructed net mass balance for Peyto Glacier, Alberta 1673–1994 (Watson and Luckman 2004b)

7.3.1.1 Extratropical Pacific Ocean

We use temperature reconstructions from coastal Gulf of Alaska and northern Patagonia to investigate past changes in the decadal oscillatory modes across the Pacific domain (Boxes 7.1 and 7.3). Wiles et al. (1998) presented a well-verified reconstruction of spring (MAM, March–May) temperature variations, based on three ring-width chronologies from coastal sites along the Gulf of Alaska, dating from 1600 to 1988. This reconstruction explains 34% of the variance in the instrumental temperature data. The decade-long variations in this reconstruction are consistent with changes in the Aleutian low-pressure system, which in turn is affected by ENSO (Dettinger et al. 2001). Spectral analysis of the temperature reconstruction shows significant peaks consistent with the ENSO-like bandwidth

(7, 8, 11, and 19 years). The reconstructed spring temperature series suggests that the recent warming exceeds temperature levels of prior centuries, extending back to AD 1600 (Wiles at al. 1998). The three coldest intervals in the spring series occurred in the seventeenth century. This cooling is consistent with the glacial record from coastal Alaska, which shows a strong advance during the late seventeenth to mid-eighteenth centuries (Wiles and Calkin 1994; Wiles 1997; Wiles et al. 2004).

A critical appraisal of surface air temperature from station records has recently been presented for southern South America (Villalba et al. 2003). Two different spatial temperature patterns were recognized in the southern Andes during the twentieth century: (1) surface cooling from 1930 to 1976 at the stations located in the northern sector of the southern Andes by the Pacific Coast (37°–42°S), and (2) a remarkable surface warming in the southern stations (south of 46°S), which intensifies at higher latitudes. Changes in the Pacific Decadal Mode around 1976 were seen in summer temperature records at most stations in the Pacific domain, starting a period with increased temperature across the southern Andes and at higher latitudes. Tree-ring records from upper tree line were used to reconstruct past temperature fluctuations for the two dominant patterns over the southern Andes. The resulting reconstructions for the northern and southern sectors of the southern Andes explain 55% and 45%, respectively, of the temperature variance over the interval 1930–1989. Cross-spectral analysis of actual and reconstructed temperatures over the common interval 1930–1989, indicates that most of the explained variance is at periods >10 years in length. Consequently, these reconstructions are especially useful for studying multidecadal temperature variations in the South American sector of the Southern Hemisphere over the past 360 years. These reconstructions show that temperatures during the twentieth century have been anomalously warm across the southern Andes. The mean annual temperatures for the northern and southern sectors during the interval 1900–1990 are 0.53°C and 0.86°C above the 1640–1899 means, respectively (Villalba et al. 2003).

Box 7.3 Climate signals in Patagonian upper-elevation tree-ring records

A great deal of progress has been made in increasing the number of upper-elevation tree-ring chronologies across the southern Andes during the past decade. This work has involved the development of more than 90 chronologies from collections of *Nothofagus pumilio*, the dominant subalpine tree in the Andes of Chile and Argentina (Villalba et al. 1997; Lara et al. 2001; Aravena et al. 2002; Villalba et al. 2003; Lara et al. 2005). These new collections have increased both the spatial coverage (ca. 35°35′ to 55°S) and the temporal span of upper-elevation records across the southern Andes (Box Fig. 7.5). The broad latitudinal distribution of *N. pumilio* across 2000 km in a north-south direction provides the opportunity to examine the relationships between *N. pumilio* growth and climate along a temperature gradient from the subtropical central Andes to the sub-Antarctic Tierra del Fuego.

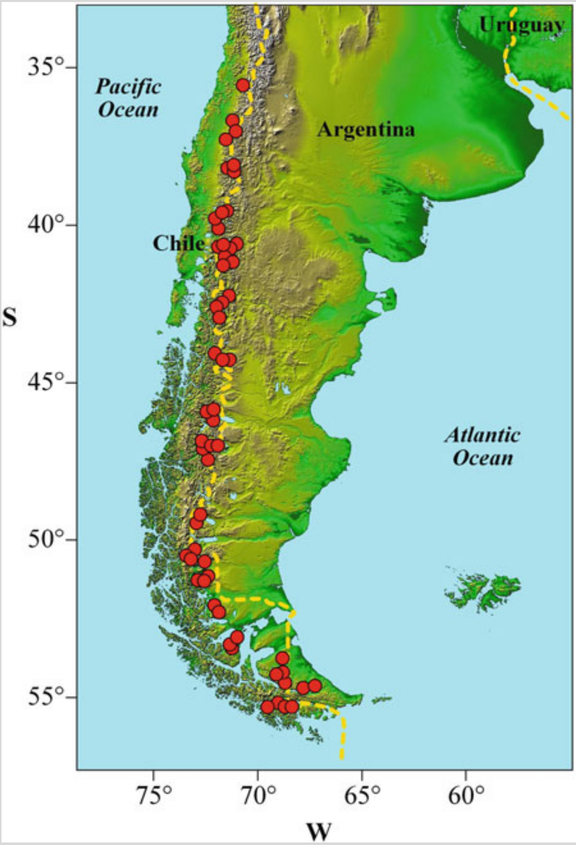

Box Fig. 7.5 *Nothofagus pumilio* chronologies in the Patagonian Andes

Nothofagus chronologies from upper tree line have been used to reconstruct past temperature fluctuations for the northern and southern sectors of the southern Andes. The reconstructions describe a well-defined cold interval from ~1640 to 1850, which conforms with the consensus view of the 'Little Ice Age' (LIA), a term commonly used to describe these cold episodes on a global scale (Bradley and Jones 1992).

Relationships between temperature reconstructions in southern South America and sea surface temperatures (SSTs) in the South Pacific and South

Atlantic Oceans clearly show that the temperature reconstructions contain information about climate variability extending over much of the tropical-subtropical Pacific and over the south Atlantic to Africa. The correlation fields between the reconstructions and SST (Box Fig. 7.6) are reminiscent of some of the global modes of SST recently derived from instrumental records. The spatial amplitudes obtained by correlating the northern Patagonian reconstruction with SSTs closely resemble the Southern Hemisphere counterpart of the interdecadal mode of the Pacific SST variability identified by Garreaud and Batistti (1999) and Enfield and Mestas-Nuñez (2000). Consistent with the documented decadal oscillatory mode of Pacific SST, the spatial field of correlations is characterized by anomalies in the western Pacific that extent to the southeast into subtropical South America. The spatial pattern that results from comparing the southern Andes reconstruction and SSTs resembles the 'global warming' mode identified by Enfield and Mestas-Nuñez (2000). According to these authors, the 'global warming' mode is the ocean counterpart to the global warming seen in surface air temperatures (SATs).

—R. Villalba, A. Lara, and M. Masiokas

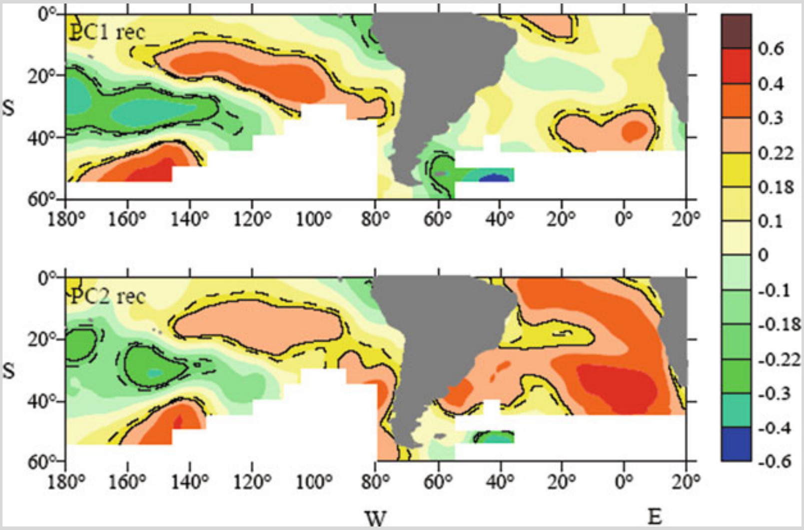

Box Fig. 7.6 Spatial correlation patterns (1857–1989) between sea surface temperature (SST) anomalies over the south Pacific and south Atlantic Oceans and the temperature reconstructions for the northern and southern sectors of the southern Patagonian Andes

The Gulf of Alaska and southern Andes reconstructions clearly show the well-documented transition from cold to warm conditions over the tropical Pacific in 1976 and are consistent with regional temperature compilations. This result reflects a comparable sensitivity of the temperature records to SST changes in the Pacific Ocean during recent decades. If decadal timescale variations in climate forced by the tropical Pacific had also affected temperature changes in the past, tree-ring-based reconstructions of temperature along the coast of North and South America should present similar oscillatory patterns. Indeed, for the common interval 1640–1989, reconstructed temperature variations from the Gulf of Alaska are significantly correlated with those of northern ($r = 0.42$, $p < 0.01$; Fig. 7.5) and southern Patagonia ($r = 0.38$, $p < 0.01$). Spatial patterns obtained by correlating the Alaska and northern Patagonia temperature reconstructions with SSTs across the Pacific and Atlantic

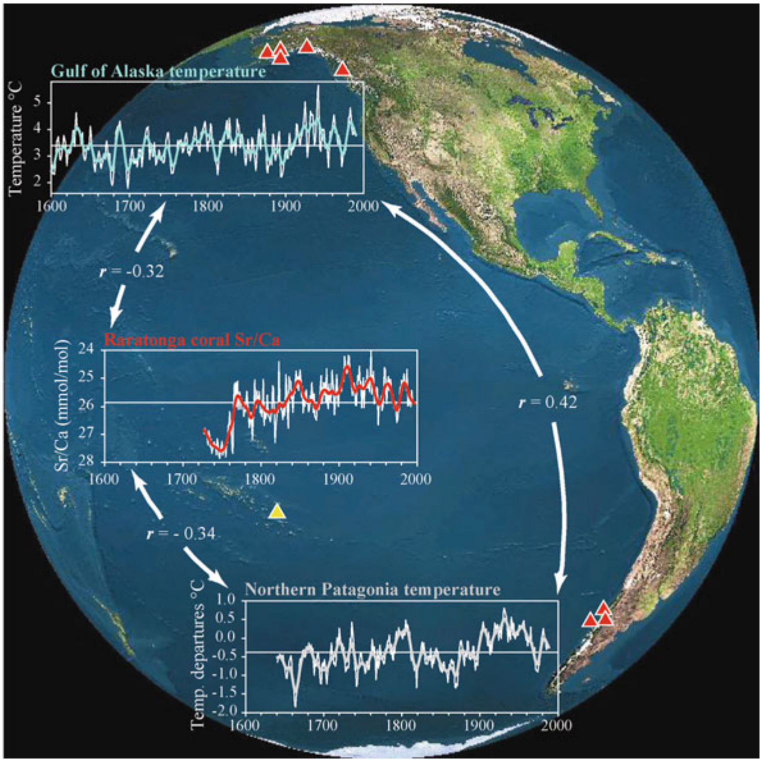

Fig. 7.5 This figure compares temperature-sensitive tree-ring records (*red triangles*) from high-latitude, western North and South America with a geochemical coral record (*yellow triangle*) from Raratonga, in the tropical South Pacific during the past three to four centuries. The series shown from top to bottom are: spring/summer Gulf of Alaska temperature reconstruction (1600–1994; Wiles et al. 1998), Sr/Ca coral record from Rarotonga (1726–1996; Linsley et al. 2004), and annual northern Patagonia temperature reconstruction (1641–1989; Villalba et al. 2003). Correlation coefficients between records are indicated. To facilitate the comparison, the Sr/Ca coral record is shown inverted

Oceans (Villalba et al. 2001) closely resemble those observed for the decadal mode of Pacific SST variability identified by Zhang et al. (1997) and Garreaud and Battisti (1999). Temperature anomalies related to ENSO-like variations are larger and more spatially consistent in northern than in southern Patagonia (Fig. 7.3c), reflecting the decrease in correlation between Alaskan and Patagonian records with increasing southern latitudes.

The Gulf of Alaska and northern Patagonia temperature reconstructions are displayed in Fig. 7.6, along with the waveforms of the two oscillatory modes that are

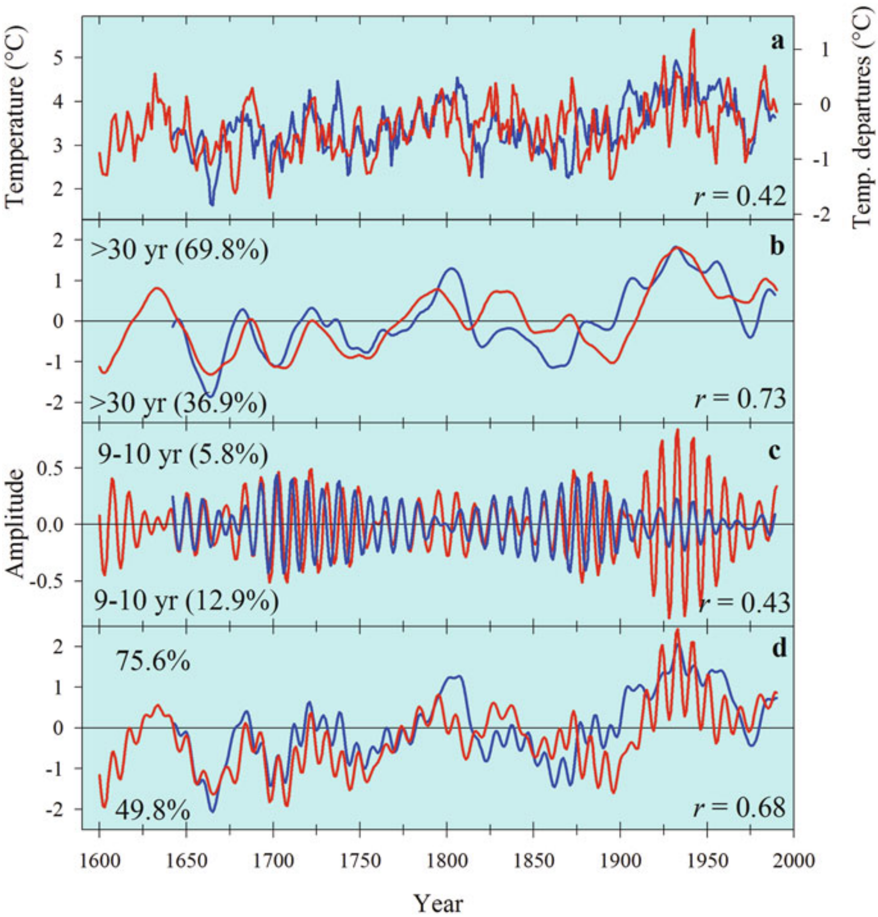

Fig. 7.6 Comparison of temperature reconstructions from northern Patagonia (*blue line*) and coastal Alaska (*red line*) and their dominant oscillations isolated by using singular spectrum analysis (SSA; panel **a**; Vautard 1995). Common oscillatory modes in both records have periods of (**b**) > 30 years, and (**c**) 9–10 years. Percentages of the original variance contributed by Patagonian and Alaskan waveforms are indicated in the upper and lower left corners, respectively. The Pearson's correlation coefficient, *r*, between the series, is shown in the lower far right. Time series included in (**d**) represent the sum of the oscillations shown in (**b**) and (**c**)

the major contributors to the common variance between these records. Waveforms were extracted from the original reconstructions by using singular spectrum analysis (SSA), basically a statistical technique related to EOF analysis, to determine oscillatory modes in the time domain (Vautard and Ghil 1989). The reconstructed waveforms, representing oscillations >30 years and approximately 10 years, reveal interesting changes in amplitude during the past 350 years. As was previously noted (Villalba et al. 2001), the temporal evolution of these components is more closely related in amplitude and intensity from 1640 to approximately 1850. After 1850, relationships between waveforms are weaker. The most remarkable feature in the long-term oscillations is the positive amplitudes during the past 100 years, reflecting the warming in the twentieth century.

7.3.1.2 Tropical Pacific Ocean

Although the temperature reconstructions from the Gulf of Alaska and northern Patagonia provide insight into the temporal evolution of the relationships between the tropical ocean and higher latitudes in the Americas, it is important to note that the variability in the records is related to tropical teleconnections along the western coasts of the Americas and not to direct forcing from the equatorial Pacific. In a first attempt to connect the extratropical tree-ring records from North and South America with climate variability in the tropical Pacific, we compared the temperature reconstructions with high-resolution coral records in the Pacific Ocean.

Long-lived corals provide continuous, high-resolution records of tropical Pacific climate that supplement the instrumental record of climate from this key region. Modern coral records from the central tropical Pacific are several centuries in length and have yielded insights into the recent history of tropical Pacific climate variability on a variety of timescales. The $\delta^{18}O$ and Sr/Ca time series from corals in the subtropical Pacific at Rarotonga (21°14′S and 159°49′W), have recently been compared with indices of climate variability in the north Pacific, suggesting some degree of cross-hemispheric symmetry of interdecadal oceanographic variability in the past centuries (Linsley et al. 2004). A tree-ring reconstruction of the north Pacific index, a measure of the intensity of the large-scale atmospheric circulation related to the Aleutian low-pressure cell, correlates significantly during the twentieth century with both instrumental tropical climate indices and a coral-based reconstruction of an optimal tropical index for the Indian and Pacific Oceans, supporting evidence for a tropical/north Pacific link that extends as far west as the western Indian Ocean (D’Arrigo et al. 2005).

The coral skeletal Sr/Ca at Rarotonga appears to be related to SST variability on annual through at least decadal timescales based on correlation with instrumental SST (Linsley et al. 2004). The coral record, which covers the period 1726–1997, is significantly correlated with both the Gulf of Alaska ($r = -0.32$, $p < 0.01$) and northern Patagonia ($r = -0.34$, $p < 0.01$) temperature reconstructions (Fig. 7.5). The low-pass fraction for each time series was isolated by using SSA (Vautard 1995), and all reconstructed components with mean frequencies longer than 20 years were summed. The results are shown in Fig. 7.7. The subtropical

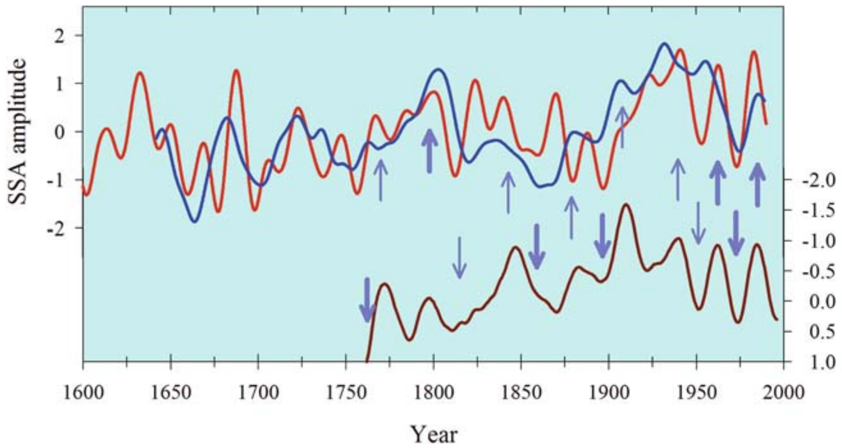

Fig. 7.7 Interdecadal to centennial variability in temperature-sensitive series from Gulf of Alaska (*red line*), northern Patagonia (*blue line*), and Raratonga (*brown line*), isolated by using singular spectrum analysis (SSA; Vautard 1995). For each record, all SSA-reconstructed components with mean frequencies longer than 20 years were summed. *Thin* and *thick arrows* indicate coincidences in oscillations between the Raratonga and one or two high-latitude records, respectively

Pacific records indicate that some of the interdecadal transitions in coral Sr/Ca temporally align with comparable transitions in the Gulf of Alaska and northern Patagonia temperature reconstructions. The remarkable shift in tropical Pacific climate during the mid-1970s is clearly captured by all three records. However, some differences are observed between interdecadal oscillations in the subtropical coral and the North and South American tree-ring records. Interdecadal temperature oscillations in northern Patagonia closely align with transitions in the Pacific coral Sr/Ca records from the 1850s to the beginning of the twentieth century, whereas the Gulf of Alaska oscillations align better with Rarotonga Sr/Ca during the second half of the twentieth century.

7.3.1.3 High-Latitude Oscillations

As was indicated in Section 7.2.3, temperature variations in high latitudes of the Northern and Southern Hemispheres are also related to changes in the NAM and SAM, respectively (Thompson and Wallace 2000; Thompson and Solomon 2002). We search for common patterns in temperature variations in the sub-Artic and sub-Antarctic regions, which in turn might provide insight on common forcings of high-latitude past climates in both hemispheres. Boreal tree-ring records from high latitudes in the Northern Hemisphere were used to provide a long-term perspective of Arctic annual temperatures (D'Arrigo and Jacoby 1993). The reconstruction was based on 12 chronologies from North America: 3 in Alaska north of 67°N, 4 in northwestern-central Canada from the Yukon to Churchill, and 5 in eastern Canada. This sub-Arctic network was complemented with five boreal

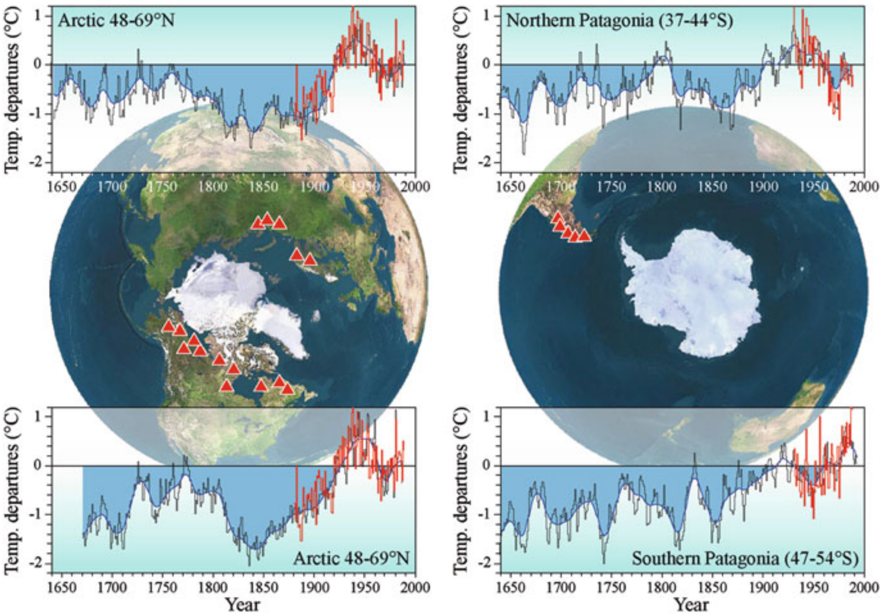

Fig. 7.8 Temperature reconstructions from Arctic and sub-Antarctic regions. The geographical locations of tree-ring chronologies (*red triangles*) used for developing the temperature reconstructions for the Arctic (*left*) and sub-Antarctic (*right*) regions are shown. See text for reconstruction details

tree-ring chronologies from Scandinavia (67°–69°N) and three from the northern Ural Mountains (Fig. 7.8). The total variance in temperature variations explained by the tree-ring chronologies during the 1880–1969 calibration period is 66%. The major low-frequency trends in the reconstructed Arctic temperatures include a cooling in the late 1600s to early 1700s, a relative warming in the 1700s, an abrupt decline in temperature in the early 1800s, a gradual warming since the middle to late 1800s, and unprecedented warming during the twentieth century. Recently, a new reconstruction of temperature variability for the Arctic has been developed with significantly improved geographical coverage and replication than previously (Gordon Jacoby, in preparation). The new temperature record reproduces most climatic events previously reconstructed, reinforcing the occurrence of major temperature changes in the sub-Arctic during the past four centuries. For comparison with the sub-Antarctic temperatures, the two reconstructions were averaged in a single Arctic temperature record.

The northern latitude record was compared with the temperature reconstructions for northern and southern Patagonia (Villalba et al. 2003, Fig. 8). For the common interval 1670–1987, the correlation coefficient between the Arctic and sub-Antarctic (average of the two southern reconstructions) is $r = 0.55$ ($p < 0.001$). For the past 400 years, striking similarities in temperature fluctuations are observed in both regions. The records exhibit their largest common variances at low frequencies

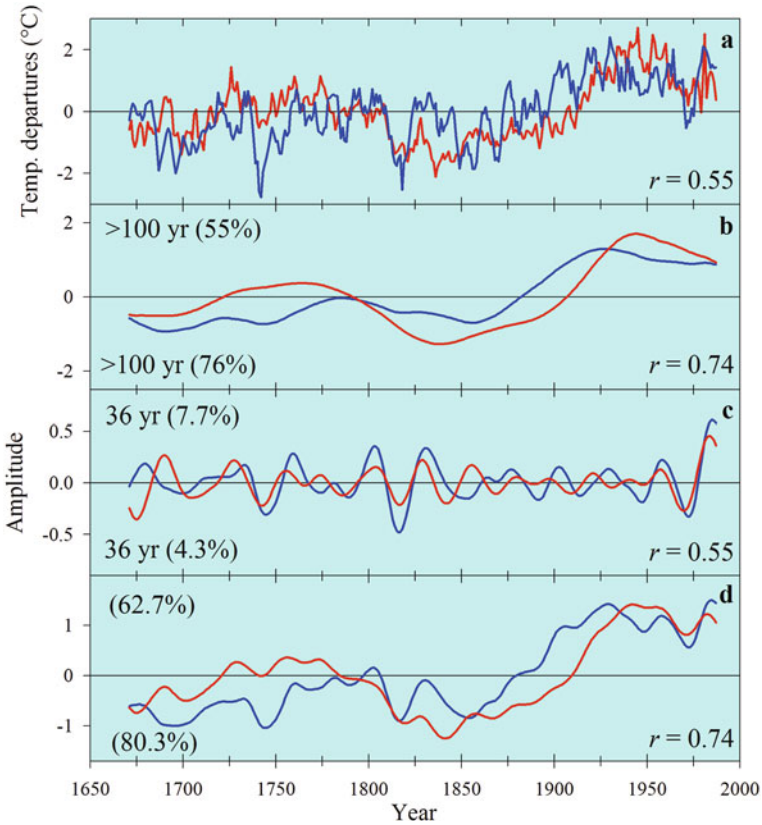

Fig. 7.9 Comparison of the amplitudes from the first principal components of the temperature reconstructions from Patagonia (*blue line*) and the Arctic (*red line*). The Patagonian and the Arctic records were obtained by averaging the temperature reconstructions shown in Fig. 7.8. Common oscillatory modes in both records have periods of (**b**) > 100 years, and (**c**) around 36 years. Time series included in (**d**) represent the sum of the oscillations shown in (**b**) and (**c**) (for explanation of the data in each panel of this figure see Fig. 7.6)

(Fig. 7.9). In both records, positive levels during twentieth-century periods exceed values back to 1670. An abrupt decrease in temperature in both regions is recorded in the 1810s, quite likely related to a series of large tropical volcanic eruptions, including an unknown source in 1809, Soufriere in 1812, and Tambora in 1815, among others (Zielinski 2000). A notable feature of temperature change revealed by the high-latitude records is the continuous transition from anomalous cold conditions in the mid-nineteenth century to anomalous warm conditions in the mid-twentieth century. In contrast, the global and hemispheric mean instrumental temperatures show almost no trend between the late 1850s and the 1910s (Jones and Moberg 2003), suggesting that high latitudes in both hemispheres share common patterns of temperature changes that are not seen at global scales.

7.3.2 Precipitation-Sensitive Records

Tree-ring chronologies from precipitation-sensitive regions across the western Americas, such as the southern United States, the Bolivian Altiplano, and central Chile, reveal common interannual to decadal-scale oscillations in precipitation variations during the past centuries (Boxes 7.4, 7.5, 7.6, 7.7 and 7.8). Spatial correlation patterns between precipitation-sensitive records and SST also show that variations in these records are strongly connected with SST anomalies in the equatorial Pacific and off the western coast of the subtropical Americas (Villalba et al. 2001).

Box 7.4 Spatial patterns of drought and wetness regimes over western North America

The network of moisture-sensitive tree-ring chronologies now available for North America has been used to reconstruct the summer (June–July–August, JJA) Palmer Drought Severity Index (PDSI) for 1200 years on 286 grid points extending from southern Mexico across the United States into southern Canada (Cook et al. 2004). These reconstructions have high temporal and spatial fidelity when compared with instrumental PDSIs on annual and decadal timescales. The average of all 286 grid points for North America indicates that the driest single year in the past 500 years occurred in 1864, and the wettest single year occurred in 1833 (Box Figs. 7.7 and 7.8). The reconstructions indicate that the twentieth century was relatively moist compared with the past 500 years, the severe Dust Bowl and 1950s droughts notwithstanding (Box Fig. 7.7).

The long-range climate influence of the El Niño/Southern Oscillation (ENSO) over western North America during the late nineteenth and twentieth centuries has been strongest in the Texas-Mexican sector of northern Mexico and the southwestern United States, with drought during La Niña events and wetness during El Niño events. The epicenter of reconstructed decadal drought was often located in the ENSO teleconnection province over the Southwest, implicating the tropical Pacific in these decadal dry regimes. The pluvials of the past 500 years were spatially heterogeneous and did not tend to recur in the ENSO teleconnection region. The notable exception was the early twentieth-century pluvial (Box Fig. 7.7), one of most extremely wet decades in 500 years, and which was concentrated in the drainage basin of the Colorado River. This period of exceptional wetness inflated expectations of surface water supplies in the Southwest, and provides a modern demonstration of the significant environmental and socioeconomic impacts associated with these decadal droughts and pluvials. The seventeenth-century Pueblo Drought lasted at least six years over the same region impacted by the twentieth-century pluvial (Box Fig. 7.7), and provides a compelling contrast to the pluvial and a strong analog for the recent multiyear drought that has severely impacted surface water supplies in the Southwest (1999–2006). Socioeconomically, the seventeenth-century Pueblo Drought caused starvation, death, and the permanent abandonment of five Pueblo communities and other villages in New Mexico.

—D.W. Stahle and E.R. Cook

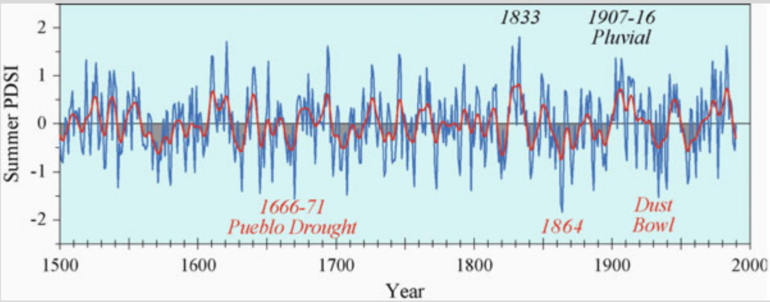

Box Fig. 7.7 North American summer Palmer Drought Severity Index (PDSI), a time series average of reconstructed PDSI from all 286 grid points over North America

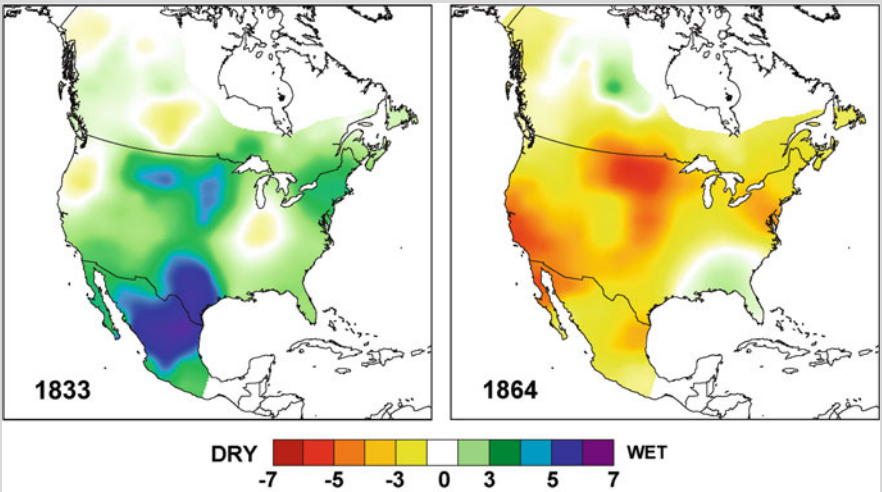

Box Fig. 7.8 Reconstructed summer Palmer Drought Severity Index (PDSI) for the wettest (1833) and driest (1864) single years in the 'North America summer PDSI' series (Box Fig. 7.7), showing the continental scale of these record moisture anomalies

Box 7.5 Western United States droughts in medieval times linked to changes over the Pacific basin

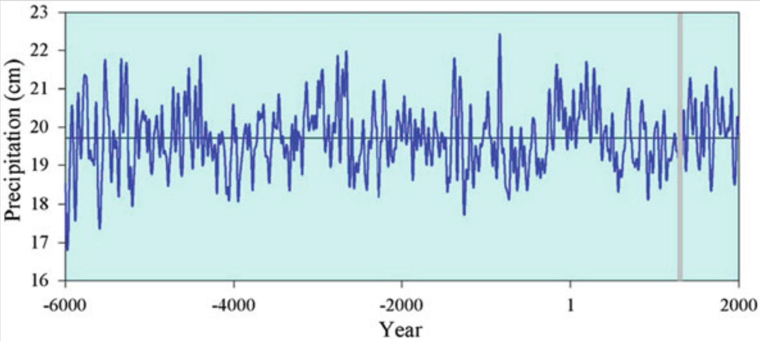

Box Fig. 7.9 Reconstructed Nevada division 3 July–June precipitation (smoothed with 50-year Gaussian filter). *Gray line* marks the transition at ~AD 1400

Several multicentury shifts in precipitation over the central Great Basin in the United States are seen in an ~8000-year reconstruction from the bristlecone pine chronology at Methuselah Walk, and in an ~1800-year reconstruction based on this and five other chronologies (Hughes and Funkhouser 1998). A remarkable, but not unique, transition from drier to wet conditions is reconstructed between the periods AD 400–1400 and AD 1400–2000 (Box Fig. 7.9). We set out to find an explanation for this transition (Graham et al. 2007). Proxy evidence from tree-ring and pollen-based reconstructions, and ocean core isotopic data suggest that the circa 1400 transition was marked by warming sea surface temperatures (SSTs) along the central California coast (Kennett and Kennett 2000; Box Fig. 7.10, plot labeled Santa Barbara Basin SST), and increasing winter precipitation with cooler summer temperatures from southern and central California into the Great Basin (Box Fig. 7.10, top plot). In today's climate, such changes are associated with El Niño episodes, suggesting the possibility that El Niño-like changes in tropical Pacific SSTs may have played a causal role in producing the mid-latitude changes suggested by the proxy records. A coral-based Niño-3.4 SST reconstruction from Palmyra Atoll in the central tropical Pacific (Box Fig. 7.10, plot 5; Cobb et al. 2003 and a foram Mg/Ca based SST reconstruction from near Mindanao in the northwest equatorial Pacific (Box Fig. 7.10, middle plot; Stott et al. 2004) support the idea of a trend towards more El Niño–like conditions at the circa 1400 transition. Analysis of the proportion of terrestrial material in a marine core taken off the coast of central Peru indicates a contemporaneous increase in river discharge associated with high-flow events (Rein et al. 2004). This picture would be consistent with the Pacific-wide pattern proposed here. Hence, it is suggested that the proxy-inferred warming of California coastal SSTs and increasing western US precipitation around, roughly, AD 1400 resulted (at least in part) from increasing tropical Pacific SSTs and resulting changes in tropical precipitation patterns. The question now arises whether other transitions in the Nevada record (for example, around 400 BC, and in the converse direction around AD 400) have similar causes.

—Nicholas E. Graham and Malcolm K. Hughes

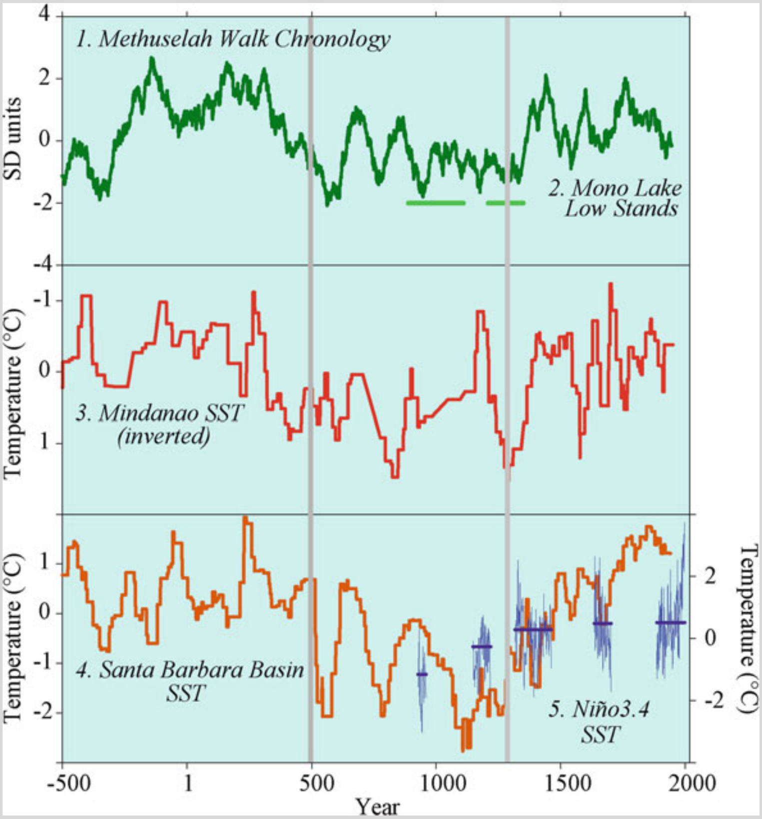

Box Fig. 7.10 Proxy records from areas in the equatorial Pacific Ocean and its eastern margin (western North America) since 500 BC. *Top Plot*: extent of Mono Lake low stands (Stine 1994) green horizontal lines, and a long tree-ring chronology from the White Mountains of California. *Middle plot*: Mg/Ca-based SST reconstruction from foraminifera near Mindanao in the northwest equatorial Pacific. Scale inverted for comparison. *Bottom Plot*: yearly values and period means (*horizontal blue lines*) of sea surface temperature (SST) (After Graham et al. 2007)

In 1999, a gridded network of 154 Palmer Drought Severity Index reconstructions for the continental United States was generated from a set of 388 tree-ring chronologies (Cook et al. 1999). More recently, the spatial and temporal coverage of the PDSI reconstructions was expanded, including 286 points in a 2.5° × 2.5° grid covering most of North America (Cook et al. 2004; Box 7.4). The new PDSI reconstructions are based on an expanded network of 835 tree-ring chronologies. The temporal coverage was also expanded to the maximum permitted by the available tree-ring data, extending back nearly 2000 years for some locations. Finally, the process of variance restoration applied to the grid point reconstructions allows for updates of those records to AD 2003 with instrumental PDSI data. In a previous work (Villalba et al. 2001), the temporal evolution of the PDSI in four cells located in the midwestern-southwestern United States were compared with precipitation-sensitive chronologies from central Chile. For the common interval 1700–1978, the correlation coefficient between the first Principal Component (PC) from the four PDSI reconstructions and tree-ring variations at El Asiento, central Chile, is $r = 0.32$ ($p < 0.001$), which was considered as an indication of common modes of variations in these series. With the increasing number of PDSI reconstructions across North America, the use of a spatial approach to study large-scale atmospheric variations connecting mid- to high-latitude precipitation changes in North and South America now appears to be feasible.

A major advance in the effort to expand the spatial coverage of tree-ring records across the Americas has been the recent development of *Polylepis tarapacana* chronologies in the Bolivian Altiplano (Argollo et al. 2004). These records, located between 17° and 20°S and above 4500 m elevation, represent the closest-to-equator tree rings in the Andes and the highest-elevation chronologies worldwide (Box 7.7). A careful examination of interannual variations in ring width and climate in the Altiplano indicate that the growth of *Polylepis* is remarkably associated with summer water balance. Most *Polylepis* records cover the past three to four centuries, but some of them extend over seven centuries. Two of the longest chronologies (Caquella and Soniquera) were merged in a single record and used for comparison with precipitation-sensitive records in other regions of the western Americas. For central Chile, a ring-width chronology from *Austrocedrus chilensis* D. Don at El Asiento (32º40′S), which represents the northernmost extent of this species in central Chile, was used for comparison with North American records (Box 7.9). Recently, the site was revisited, and series from the new cores were merged with the original data collected in 1974 by LaMarche (1975).

Box 7.6 A network of tree-ring chronologies for northern and central Mexico

The mixed conifer forests and riparian areas of northern and central Mexico contain some of the most climate-sensitive species in the North American region (Box Fig. 7.11). Douglas-fir (*Pseudotsuga menziesii*) is one of these species that has been widely recognized due to its sensitivity to climate (Fritts 1976). Douglas-fir has a native latitudinal range covering at least 38° in the Northern Hemisphere and extending well into southern Mexico at latitudes below 17°N. In Mexico, Douglas-fir occurs in scattered insolated populations of mixed conifer forests located at high elevations, thriving in cool microenvironments and scarped terrains of the Sierras Madre Occidental and Oriental (Martínez 1963). The annual ring of this species is anatomically divided into two distinct layers: the earlywood (EW) is composed of low-density, light-colored cells, whereas the latewood (LW) has smaller, darker cells with thicker walls. The development of separate EW and LW chronologies provides more information on the influence of intra-annual climate variability than using total ring width data (Cleaveland 1986; Stahle et al. 1998).

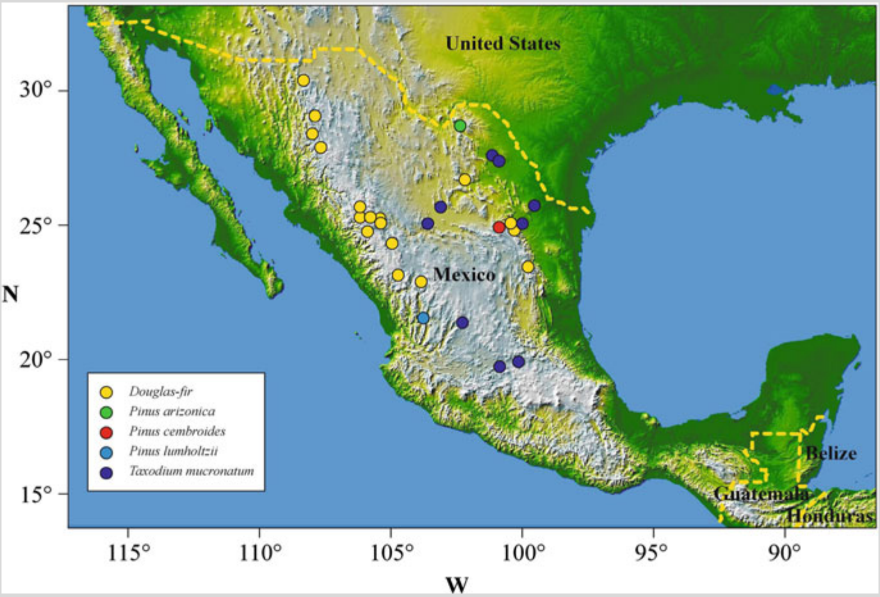

Box Fig. 7.11 Tree-ring chronologies in Mexico

Ahuehuete or Montezuma bald cypress (*Taxodium mucronatum*), a widely distributed riparian species that is considered to be the national tree of Mexico, has been used to develop the longest tree-ring chronologies in Mexico. In recent years, over 30 new tree-ring chronologies have been developed or are in process as part of the CRN03-IAI project. The Douglas-fir chronologies range between 129 and 604 years, bald cypress between 117 and 1550 years, and pinyon pine (*Pinus cembroides*) over 400 years. Some available Douglas-fir and bald cypress chronologies are being extended with the use of cross sections from subfossil wood or logged material. The EW growth of Douglas-fir trees in Mexico is influenced by dominant climatic conditions in the winter–spring period previous to growth (November to current June; Box Fig. 7.12), explaining around 70% of the variance in growth. Cool season precipitation in northern Mexico is increased by the warm phase of El Niño/Southern Oscillation (ENSO). On the other hand, the LW width is affected by the summer precipitation and the monsoon system. Annual ring width of bald cypress is influenced by the seasonal late spring to summer precipitation (June–September), explaining 52% of the variance in growth. The regions of northern and central Mexico have highly limited water resources, and paleoclimatic reconstructions are essential to understand the hydroclimatic variability that characterizes these regions. Determining past climatic variability is essential to planning proper management strategies for water use, and tree-ring studies offer the best opportunity to understand this variability over the last 1000 years.

—J. Villanueva-Diaz, J. Cerano-Paredes, D. Stahle, M. Therrell, M. Cleaveland, and B.H. Luckman

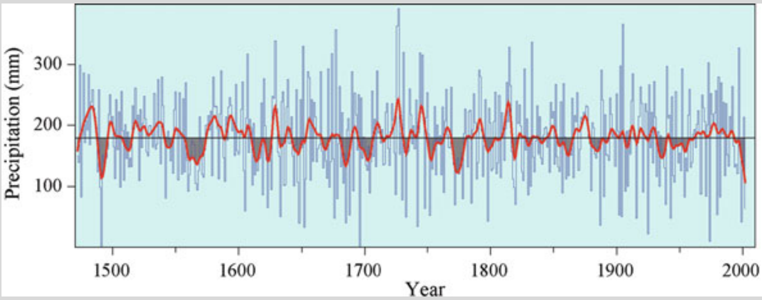

Box Fig. 7.12 The winter–spring precipitation series reconstructed from an earlywood Douglas-fir chronology in Chihuahua, Mexico. The reconstruction covers the period 1472–2002

Box 7.7 The *Polylepis tarapacana* chronologies: The highest elevation tree-ring records worldwide

Polylepis, a genus from the Rosaceae family, includes several woody species of small- to middle-sized trees that grow at very high altitudes in the tropical Andes of South America (Kessler 1995). *Polylepis tarapacana*, adapted to drier and colder conditions than other species of the same genus, reaches the highest elevation of tree growth in the world. On the slopes of the high volcanoes in Bolivia and along the Bolivian-Chilean-Argentinean border, *P. tarapacana* grows between 4100 and 5200 m elevation.

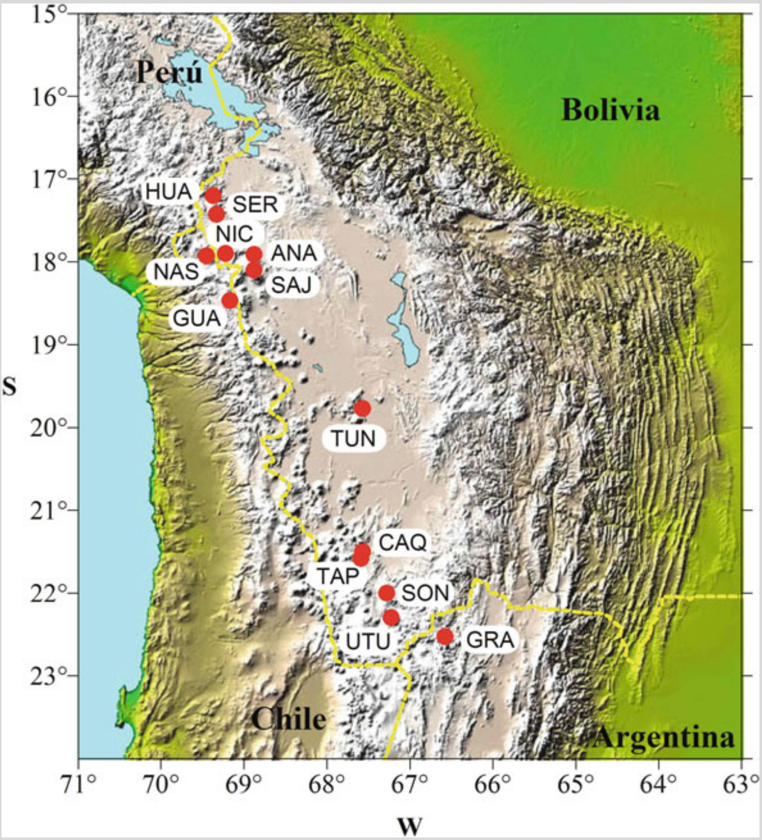

Box Fig. 7.13 *Polylepis tarapacana* chronologies in the Bolivian Altiplano and adjacent areas of Chile and Argentina. HUA: Huarinka; SER: Serke; NIC: Cerro Nicolás; ANA: Analasjchi; NAS: Nasahuento; SAJ: Sajama; GUA: Guallatire; TUN: Tunupa; CAQ: Caquella; TAP: Tapachilca; SON: Soniquera; UTU: Uturun-co; GRA: Cerro Granadas

Polylepis stands are almost exclusively restricted to volcanic slopes, with a strong preference for well-insolated north-facing slopes. Extensive collections of *P. tarapacana* were conducted in Bolivia, Chile, and Argentina (16°–22°S) as part of the IAI-CRN program to reconstruct climate variations from upper-elevation tree rings along the Americas (Box Fig. 7.13). Presently, the chronologies range between 98 and 705 years in length, and represent the highest tree-ring records worldwide (Box Fig. 7.14). In order to determine the climatic variables controlling *P. tarapacana* growth, interannual variations in tree growth were compared with regional records of precipitation and temperature. Correlation functions indicate that the radial growth of *P. tarapacana* is influenced by water balance during the summer previous to the ring formation. At the sampling sites, precipitation explains around 50% of the total variance in growth. Summer temperatures, which increase evapotranspiration and reduce soil water supply, are negatively correlated with tree growth (Argollo et al. 2004).

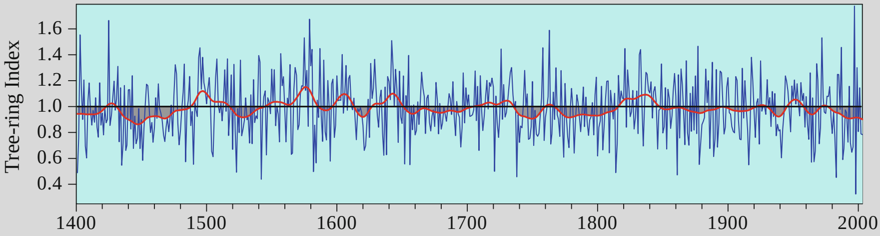

Box Fig. 7.14 Composite chronology resulting from merging the *Polylepis tarapacana* ring width series from Caquella and Soniquera in the Bolivian Altiplano

Traditionally, the wood of *Polylepis tarapacana* has been used by local populations in the Bolivian Andes for construction, particularly for house and church roofs. Wood from old buildings offers the possibility of extending the upper-elevation records of *P. tarapacana* back in time for the past millennium. These records offer the unique opportunity for reconstructing precipitation variations across the altiplano during the past five to seven centuries or more.

—Jaime Argollo, Claudia Soliz, Jorge Moya, Janette Pacajes, Mariano S. Morales, and Ricardo Villalba

7.3.2.1 Subtropical Precipitation and ENSO

Precipitation variations in the United States–Mexico, the Bolivian Altiplano, and central Chile are related to climatic changes in the tropical Pacific. It is well known that there is a strong teleconnection between SST changes in the tropical Pacific and precipitation anomalies in the southern United States and northern Mexico (Ropelewski and Halpert 1986; Kiladis and Diaz 1989; Cole and Cook 1998). Warmer SSTs in the tropical Pacific typically result in increased precipitation anomalies in this region. Spatial correlations between different indices of tropical Pacific circulation and the grid point PDSI series over the conterminous United States show that the geographic location of the highest correlation field is the southwestern United States (Cook et al. 2000), a finding that is consistent with the patterns identified by using instrumental records.

Interannual variability in precipitation over the altiplano is primarily related to changes in the mean zonal flow, reflecting changes in meridional baroclinicity between tropical and subtropical latitudes, which in turn is a response to sea surface temperature changes in the tropical Pacific (Garreaud et al. 2003). There is a general agreement that a significant fraction of interannual variability in summer precipitation is related to ENSO (e.g., Aceituno 1988; Lenters and Cook 1999; Vuille 1999; Vuille et al. 2000; Garreaud et al. 2003). All of these studies concluded that El Niño years tend to be dry, whereas La Niña years are often associated with wet conditions on the altiplano. However, dry La Niña years and wet El Niño years are not completely uncommon, which indicates that the relationship between SST anomalies in the tropical Pacific and precipitation in the central Andes is not simple (Garreaud et al. 2003). Finally, relationships between SSTs in the equatorial Pacific and precipitation anomalies in central Chile (30º−35ºS) have been reported by several authors (Quinn and Neal 1983; Aceituno 1988; Rutlland and Fuenzalida 1991; Aceituno and Montecinos 1996; Montecinos and Aceituno 2003). Positive rainfall anomalies in central Chile are associated with warmer SSTs in the tropical Pacific. Conversely, cold SSTs correspond quite closely to dry conditions in the area.

To gain insights into the long-term relationships between SST in the tropical Pacific and precipitation in the southwestern United States, the Bolivian Altiplano, and central Chile, we compared precipitation-sensitive records from these three regions with a multiproxy-based reconstruction of SST for the El Niño-3 region (Mann et al. 2000). Through exploiting the complementary information shared by a wide network of different types of proxy climate indicators, the multiproxy El Niño-3 reconstruction reduces the weaknesses in any individual type or location of indicator and makes use of the mutual strength of the diversity in the records. The reconstructed eastern equatorial Pacific Niño-3 areal-mean SST index has been previously used as a direct indication of ENSO itself for the past 400 years (Mann et al. 2000). A large proportion of the tree-ring chronologies from the southwestern United States and Mexico have been used as predictors of both the Niño-3 index and PDSI reconstructions, which make the reconstructions not statistically independent. In contrast, neither the El Asiento nor the Bolivian Altiplano chronologies have been included in the Niño-3 index reconstruction.

Box 7.8 Tree-ring chronologies from *Austrocedrus chilensis* in central Chile

Austrocedrus chilensis (D. Don, Serr et Bizz.) is the most northerly-distributed conifer species of the Andean Patagonian forests. The species occurs within a wide latitudinal range between 32º39′ and 43º40′S. The northernmost populations of the species also occupy the tree line at high elevations in the Andes of central Chile. These populations are growing on steep, rocky slopes under severe water stress in low-density, scattered stands. The trees from these marginal stands exceed 1200 years in age and exhibited typical features of long-lived species, like strip bark growth, twisted branches, and crown dieback. According to Edmund Schulman (1956), *Austrocedrus* 'was the most suitable dendrochronologic species in the southern Andes. Its ring record is as well defined as any in the drought conifers of the Rocky Mountains, and it possesses the type of cambial growth regime which leads to good crossdating quality in the ring series.'

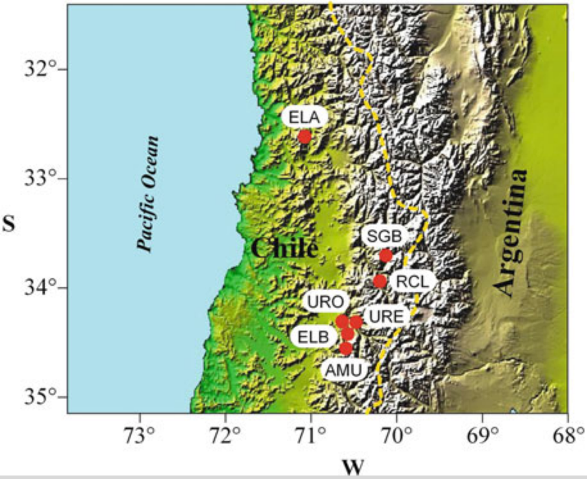

Box Fig. 7.15 *Austrocedrus chilensis* chronologies in central Chile. ELA: El Asiento; SGB: San Gabriel; RCL: Río Clarillo; URO: Urriloa Oeste; URE: Urriola Este; ELB: El Baule; AMU: Agua de la Muerte

Several tree-ring collections of *Austrocedrus chilensis* were taken in central Chile during the early years of dendrochronological studies in South America. The El Asiento site (ELA, Box Fig. 7.15) was first visited by Valmore LaMarche in 1972. After that, several collections were conducted in San Gabriel, Río Clarillo, Urriola Oeste, Urriola Este, El Baule, and Agua de la Muerte. In recent years, new collections have been carried out in these sites to update and extend these chronologies, especially by collecting preserved relict wood (Box Fig. 7.15). Correlation function analyses show a strong climatic signal related to winter–spring precipitation during the previous and current growing seasons. A composite record consisting of El Asiento and El Baule chronologies has been used by LeQuesne et al. (2006) to develop new estimates of June–December precipitation for central Chile extending from AD 1200 to 2000 (Box Fig. 7.16).

The reconstruction suggests that the decadal variability of precipitation in central Chile was greater before the twentieth century, with more intense and prolonged dry and wet episodes. Multiyear drought episodes in the eighteenth, seventeenth, sixteenth, and fourteenth centuries exceed the estimates of decadal drought during the twentieth century. The reconstruction also indicates an increase in interannual variability after 1850. In fact, the risk of drought exceeding all thresholds increases dramatically in the reconstructed precipitation series after 1850, consistent with the drying trends indicated by selected long instrumental precipitation records.

—Carlos LeQuesne and David Stahle

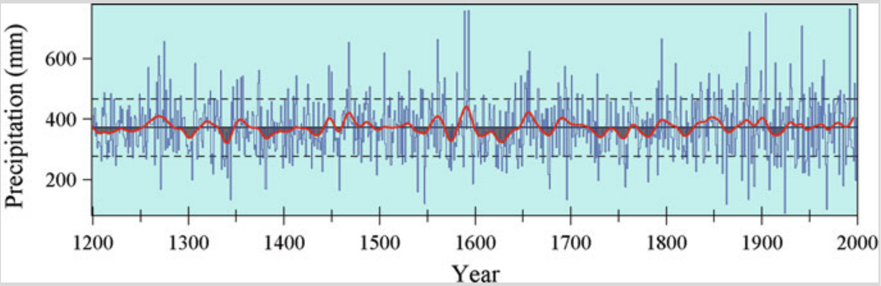

Box Fig. 7.16 Tree-ring-reconstructed precipitation for central Chile from AD 1200 to 2000. A cubic smoothing spline highlighting multidecadal variability (ca. 25 years, fit for the period 1205–1995) and the ±1.0 standard deviation thresholds are also plotted

It is important to note that based on instrumental records, the strongest teleconnections between precipitation in the southern United States–northern Mexico and SST in the tropical Pacific have been identified for the winter months (Kiladis and Diaz 1989; Stahle et al. 1998; Cleaveland et al. 2003), whereas the PSDI reconstructions are reflecting drought conditions during the summer months. On the other hand, the *Polylepis* chronologies in the Bolivian highlands and the *Austrocedrus* chronologies in central Chile are sensitive to summer and winter precipitation, respectively. Despite the limitation imposed by the differences in seasonal-window responses of trees from different regions to precipitation and the fact

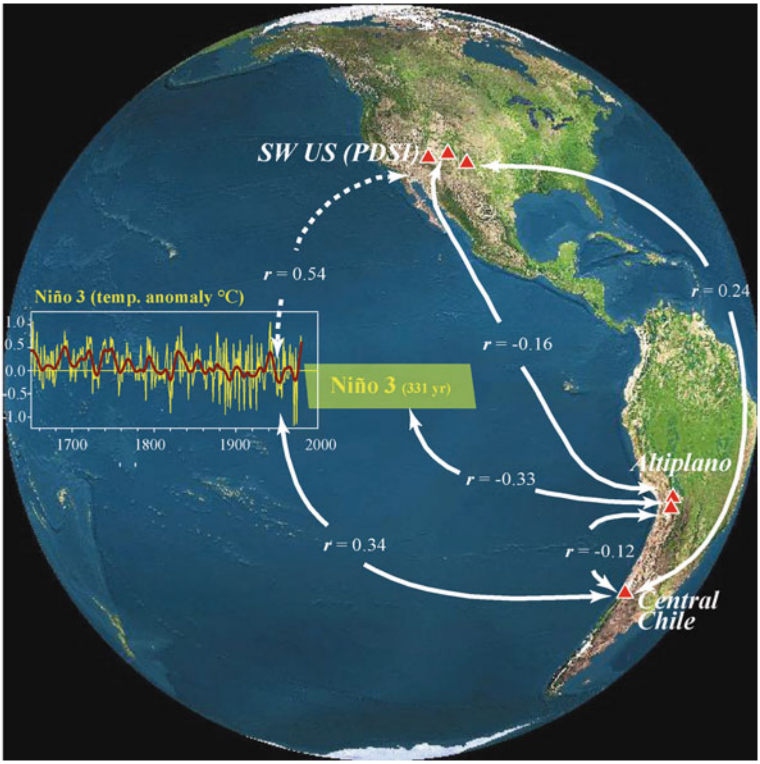

Fig. 7.10 Comparison of precipitation-sensitive tree-ring records across western America and El Niño/Southern Oscillation. The reconstruction of Niño-3 region temperature (Mann et al. 2000) was used as a proxy for tropical forcing of precipitation variations. The series used for comparison, from top to bottom, are: Tree-ring-based Palmer Drought Severity Index (PDSI) reconstructions from the southwestern United States (SW US) from Cook et al. (2004); a composite *Polylepis* record, including the Caquella and Soniquera chronologies from the Bolivian Altiplano (Argollo et al. 2004); and the El Asiento chronology in central Chile (LeQuesne et al. 2006). Correlation coefficients between records are indicated. The number of years for the comparisons is 331. The PDSI and the Niño-3 region reconstructions are not statistically independent. Some Texas-Mexican chronologies were used as predictors in both reconstructions

that we are making comparisons with an annual Niño-3 index reconstruction, the precipitation-sensitive records from the three extratropical regions in North and South America are significantly correlated with the Niño-3 index reconstruction during the 1650–1980 interval used for comparison (Fig. 7.10). The correlation coefficients between the PDSI reconstructions in the midwestern-southwestern United States and the Niño-3 index oscillate between $r = 0.20$ and $r = 0.65$. Although most correlation coefficients are remarkably high, the lack of independence between these records makes it difficult to determine the statistical significance of these relationships.

For the common interval 1650–1980, the first PC of the El Asiento chronology in year t and t+1 is significantly correlated with the Niño-3 index ($r = 0.34$, $p < 0.01$), which may be considered as a first indication of persistence in the influence of tropical SSTs on precipitation in central Chile. Long-term relationships between SST in the tropical Pacific and precipitation in the Bolivian Altiplano are also inferred from the statistically significant correlation between the two independent estimates ($r = -0.34$, $p < 0.01$).

7.3.2.2 Dominant Oscillations in Precipitation Variations

Cross-spectral analysis was used to identify coherent oscillation modes in tropical Pacific SST and precipitation variations in central Chile and the Bolivian Altiplano. Coherent oscillations between Niño-3 index and precipitation in central Chile are observed at 3.5 years, the classic El Niño frequency domain, but also at 20–28 years, an oscillation likely related to the Pacific Interdecadal Mode (Fig. 7.11). Cross-spectral analysis of the Niño-3 index and *Polylepis* records in Bolivia indicates significant coherence at 2.9, 3.2, 3.8, 8.5–10, and 19 years, a cycle also identified in the Gulf of Alaska temperature reconstructions (Fig. 7.11).

Following the previous cross-spectral analysis, we proceed to isolate the major waveforms in the precipitation-sensitive records using singular spectrum analysis (Vautard and Ghil 1989; Vautard 1995). Two dominant oscillations, representing modes of common variance at 3.6 and 28 years, were isolated from the Niño-3 and

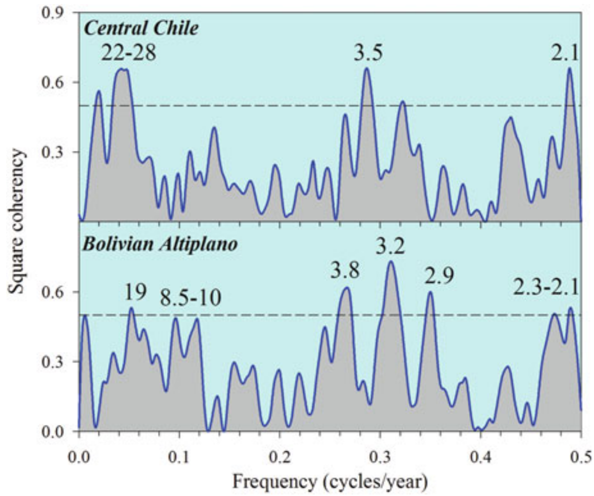

Fig. 7.11 Coherency spectra between the Niño-3 temperature reconstruction (Mann et al. 2000), and precipitation-sensitive chronologies in central Chile (*upper*) and the Bolivian Altiplano (*lower*) during the interval 1650–1981. Records are highly coherent at 3–4 years, the classic El Niño oscillations, but also at decennial-scale wavelengths longer than 10 years. *Horizontal broken lines* represent the 95% confidence level for the squared-coherency analyses. The periods are given in years for each significant coherency peak

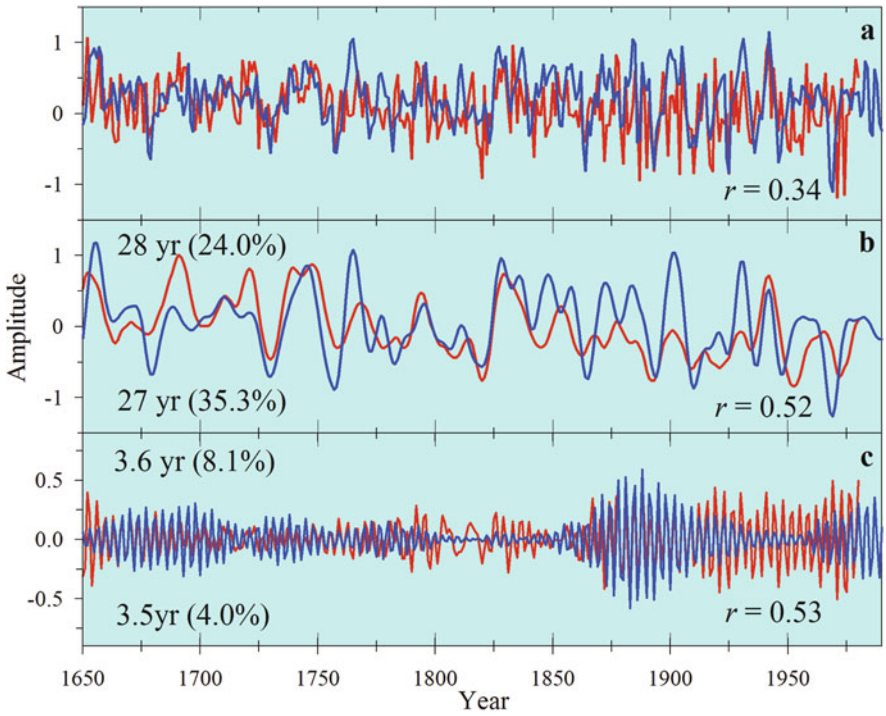

Fig. 7.12 Comparison of sea surface temperature (SST) in the tropical Pacific, represented by Niño-3 temperature reconstruction (Mann et al. 2000; *red line*), and precipitation variations in central Chile, inferred from El Asiento chronology (*blue line*), and significant correlated oscillatory modes extracted by singular spectrum analysis (SSA). Common oscillatory modes have periods of (**b**) 27–28 years, and (**c**) 3.5–3.6 years. Percentages of the original variance contributed by each of Niño-3 and El Asiento waveforms are indicated in parentheses at the upper and lower left corners of the figures, respectively. In the lower right corners, *r* is the Pearson's correlation coefficient between Niño-3 and El Asiento series. Marked increases in the interannual oscillatory modes centered at 3.6 years are observed in both series since about 1850 (**c**)

El Asiento chronology (Fig. 7.12). In general, the temporal evolution of the 28-year component shows similar fluctuations in amplitude and intensity from 1650 to 1850. After that, relationships between the 28-year waveforms are weaker. Starting around 1850, a marked increase in amplitude is observed in the 3.6-year waveforms from both the Niño-3 index and El Asiento series. Contrasting patterns in El Niño–related oscillations before and after 1850 have been noted previously by several authors (Stahle et al. 1998; Villalba et al. 2001; D'Arrigo et al. 2005).

Singular spectrum analysis of the precipitation-sensitive records from the Bolivian Altiplano also reveals common oscillatory modes with Niño-3 SST. Two major temporal patterns, centered at 3 and 4 years, are coherent with similar oscillations in tropical SSTs during the past four centuries. Similar to previous waveform comparisons, the common oscillation between the Bolivian and Niño-3 records, centered at 9.7 years, are more consistent in time and amplitude before 1850 (Fig. 7.13).

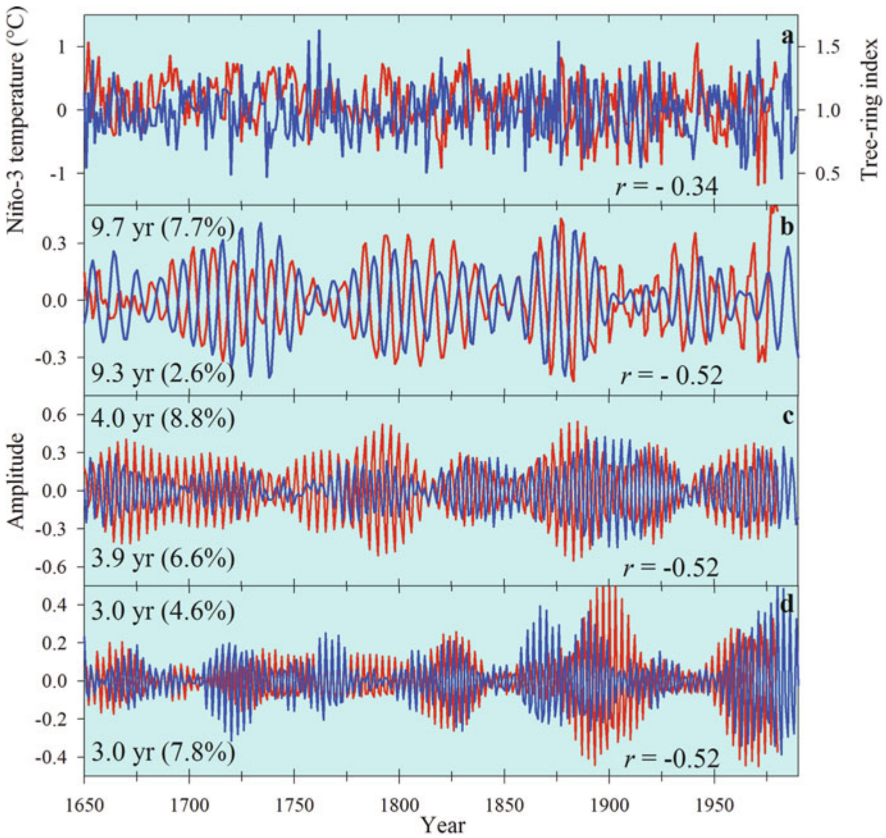

Fig. 7.13 Comparison of sea surface temperature (SST) in the tropical Pacific, represented by the Niño-3 temperature reconstruction (Mann et al. 2000; *red line*), and precipitation variations in the Bolivian Altiplano, inferred from Caquella-Soniquera composite chronology (*blue line*) lagged 1 year ($t + 1$), and significant correlated oscillatory modes extracted by singular spectrum analysis (SSA). Common oscillatory modes have periods of (**b**) 9–10 years, (**c**) 4 years, and (**d**) 3 years. Percentages of the original variance contributed by each of Niño-3 and the Bolivian waveforms are indicated in parentheses at the upper and lower left corners of the figures, respectively. In the lower right corners, r is the Pearson's correlation coefficient between Niño-3 and the Bolivian composite series

These spectral analyses basically reaffirm the existence of common oscillatory modes in tropical Pacific SST and precipitation-sensitive chronologies in subtropical North and South America, but also reveal changes in the stability of teleconnections over time. Indeed, moving correlations (using a 50-year window) between the precipitation-sensitive chronologies from South America and the El Niño-3 SST reconstruction revealed such changes in the temporal stability of the teleconnections (Fig. 7.14). Significant correlations occur for most of the sub-periods compared; however, correlation coefficients were not statistically significant during the second part of the eighteenth century between the Niño-3 SST and both the Bolivian and

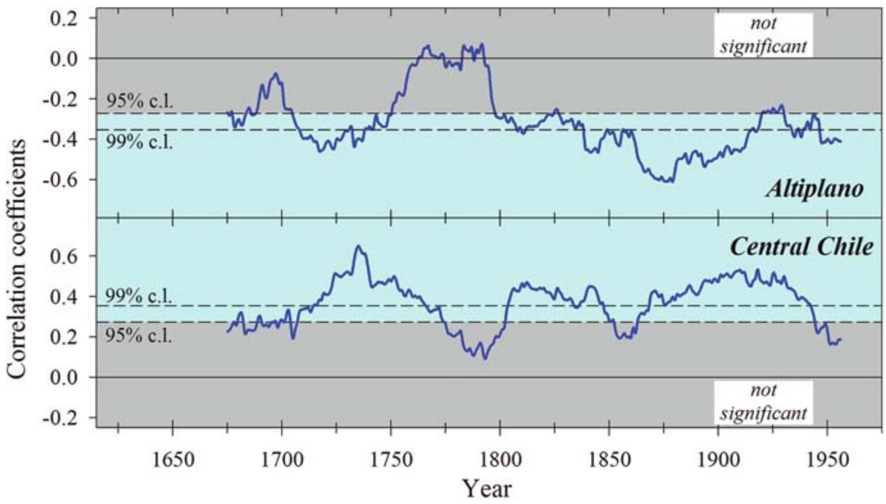

Fig. 7.14 Relationships between reconstructed Niño-3 temperature variations and interannual precipitation variability in the Bolivian Altiplano and Central Chile since 1650. Tropical influences on precipitation in both regions are evaluated by changes in the moving Pearson correlation coefficients (*blue lines*) between reconstructed Niño-3 temperatures and tree-ring width variations from *Polylepis* (*above*) and *Austrocedrus* (*below*) plotted on centroids of 50-year intervals. Lines at the 95 and 99% confidence intervals are indicated

central Chile records. This interval is characterized by low amplitudes of the interdecadal (27–28 years) oscillations in the Niño-3 and central Chile, and out-of-phase relationships in the 3- to 4-year oscillations between Niño-3 and both the central Chile and Bolivian records (Figs. 7.12 and 7.13).

The El Asiento precipitation-sensitive record from central Chile is positively correlated ($r = 0.24$ for the 350-year interval 1650–1998) with the first PC from 28 PDSI reconstructions in the midwestern-southwestern United States, the area most consistently affected by variations in tropical Pacific SST. Warm ENSO events are related to abundant precipitation in both regions. In contrast, droughts in the Bolivian Altiplano occur in years of warm ENSO events. Overall, the upper-elevation chronologies from Bolivia are consistently negatively correlated ($r = -0.16$, for the 346-year interval 1650–1998) with the first PC from 28 PDSI reconstructions from the southwestern United States and northern Mexico.

An additional indication of common ENSO influences on precipitation variations across the western Americas is provided by similarities in spatial correlation patterns between PDSI and Niño-3 index reconstructions and those resulting from the comparison between the PDSI reconstructions and precipitation-sensitive records in South America during the past 400 years. Figure 7.15 shows the teleconnection map for the Niño-3 index with reconstructed PDSI over the 1650–1980 time period common to all series. The geographical location of the highest correlation field is where one would expect based on instrumental and past proxy record analyses (Ropelewski and Halpert 1986; Kiladis and Diaz 1989; Cole and Cook 1998).

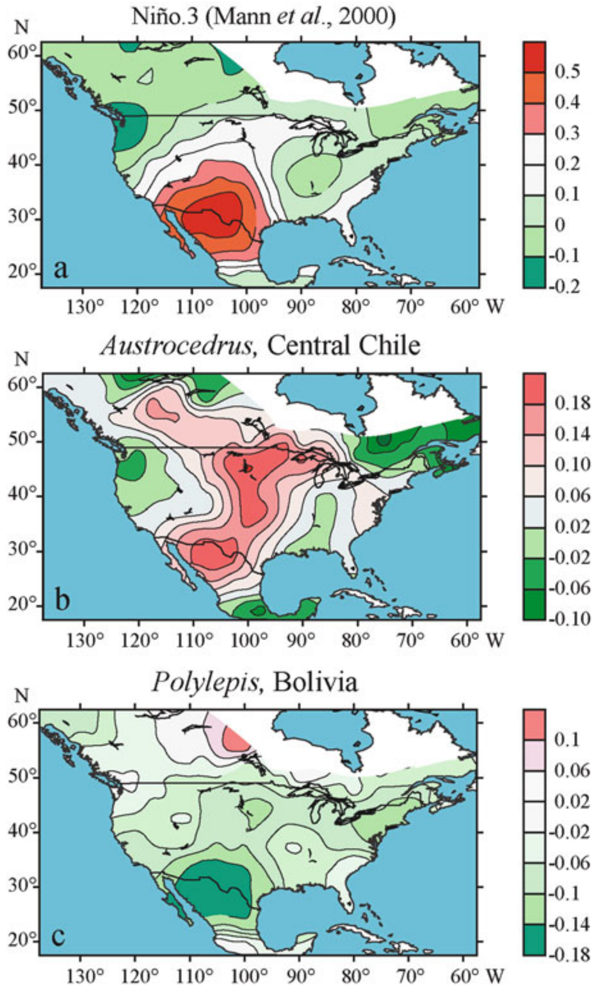

Fig. 7.15 Spatial correlation patterns between 297 Palmer Drought Severity Index (PDSI) reconstructions across North America (Cook et al. 2004) and (**a**) El Niño-3 region temperature reconstruction (Mann et al. 2000); (**b**) tree-ring variations from the precipitation-sensitive El Asiento *Austrocedrus* chronology, Central Chile; and (**c**) composite *Polylepis* chronology from Caquella and Soniquera in the Bolivian Altiplano

As was mentioned above, the tree-ring records used in the Niño-3 reconstruction are not completely independent of those used in the PDSI reconstructions, but the resulting spatial correlation pattern provides the basis for the search for commonalities with spatial patterns from comparison with the central Chile and the Bolivian Altiplano chronologies.

Figure 7.15b,c shows the spatial correlation patterns for the central Chile and altiplano chronologies with reconstructed PDSI over the 1650–1980 time period common to Niño-3 index reconstruction. Significant correlations are observed in the southwestern United States–northern Mexico for both patterns, with the sign being positive for El Asiento and negative for the *Polylepis* records. Overall, the spatial correlation patterns produced by Niño-3 index reconstructions and the precipitation-sensitive records from South America are similar, indicating that the tree-ring estimates are capturing the interhemispheric ENSO teleconnection pattern. The significant correlations between El Asiento and PDSI are more extensive and penetrate northeastward into the central and upper Midwest of the US. This extension in the correlation pattern also has been observed by using instrumental records, particularly during the first decades of the twentieth century (Cole and Cook 1998). In contrast, the spatial pattern with the Bolivian chronologies is highly concentrated to the southwestern United States–northern Mexico region, making it remarkably similar to the pattern based on the Niño-3 index (Fig. 7.15).

7.4 Future Research

The previous results highlight the potentiality of tree rings as reliable sources of information concerning past climate variations. However, dendroclimatological studies are confronted by many challenges in the western Americas. New tree-ring chronologies in subtropical Mexico (*Pseudotsuga menziesii*, *Pinus hartwegii*, *Taxodium mucronatum*, *Pinus cembroides*, *Pinus lumholtzii*), in the high-elevation tropics of Bolivia and adjacent areas of Chile and Argentina (*Polylepis tarapacana*), and subtropical Argentina (*Prosopis ferox*) allow, for the first time, studies of annual variability in the subtropics. However, these records are still sparse and difficult to develop (Box 7.9). On the other hand, the development of climate-sensitive chronologies from the seasonally dry areas of the high- and lowland tropics remains a major task in the Americas and the world. It was only during the first years of the twenty-first century that a number of exploratory studies, mainly in coastal Peru, have established the basis for building reliable and calendar-dated chronologies from *Bursera graveolens*. The chronology, which covers the interval 1950–2002, shows an ENSO signal with an average recurrence period of about 5 years (Rodriguez et al. 2005). The search for longer records from tropical species with clear, identifiable annual rings is still a major challenge in modern dendroclimatology.

An alternative to the reliance on the presence of annual rings in tropical trees is provided by isotopic studies. An improved mechanistic understanding of controls on the oxygen isotope ratio ($\delta^{18}O$) of alpha cellulose (Roden et al. 2000) and rapid processing techniques (Brendel et al. 2000) make possible the construction of high-resolution isotope series from tropical trees that can be analyzed to provide both a chronology and paleoclimatic information, even in trees lacking annual rings (Evans and Schrag 2004). The seasonal cycle in $\delta^{18}O$ of tropical montane precipitation, primarily controlled by the difference in the amount of precipitation between wet and dry seasons, is reflected in $\delta^{18}O$ of the cellulose of trees. This seasonal rhythm can then be used for chronological control. Pilot applications of these techniques in Costa Rica, Peru, and the Amazon show annual isotope cycles as great as 4–6‰, which permit high-resolution chronological control even in the absence of annual rings. Interannual variability up to 8‰ in $\delta^{18}O$ cellulose is associated with year-to year differences in precipitation amounts (Evans and Schrag 2004).

The seasonality in climate and tree growth is an important feature to be considered in the processes of interhemispheric comparisons. For example, ENSO matures during the boreal winter (austral summer) when the climatic anomalies set by the extratropical teleconnections are more marked. However, tree responses vary according to their location and biology, leading to wide variability between species in the total amount of the ENSO signal captured by trees during the growing season concurrent or following the event. There is a need for further investigation of the basic processes that bring about year-to-year variations in tree-ring properties, cell dimensions, wood chemistry, wood density, or ring width (Hartsough and Biondi 2003; Roig et al. 2003; see Box 7.9). Long-term monitoring that employs a combination of weather stations and dendrometers will better characterize both the climate to which the tree is responding and the season of wood formation, particularly in tropical trees. A better understanding of the relationship between tree growth and climate will facilitate the interpretation of the temporal climatic window recorded by trees, which in turn will result in better, ecophysiologically sound reconstructions of past climate variations.

Box 7.9 Monitoring of tree growth dynamics to improve dendroclimatic models

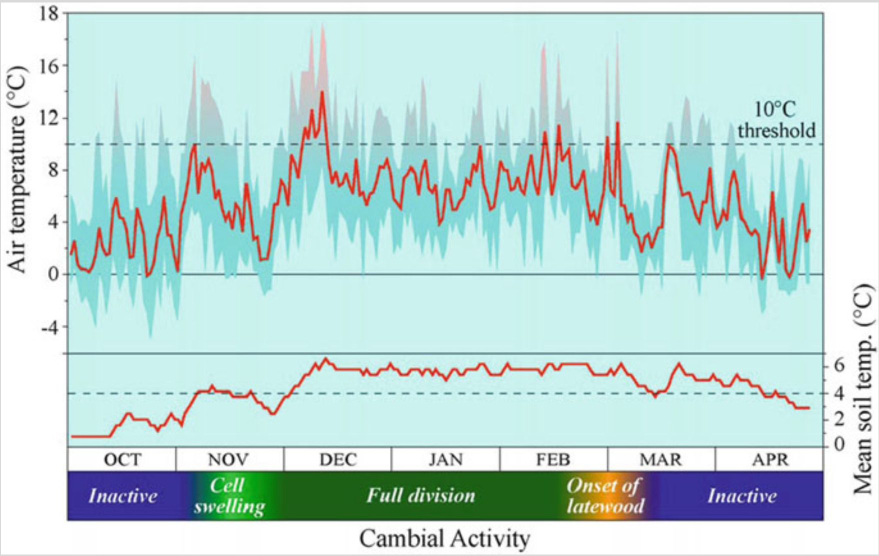

Box Fig. 7.17 Seasonal course of climate related to variations in ring morphology and leaf phenology of *Nothofagus pumilio* trees in Tierra del Fuego, as illustrated by the 2002–2003 observational period. Air temperatures are at 1.2 m above ground and soil temperatures are at 0.25 m underground (the layer with major development of the *Nothofagus* root system)

Fine-scale monitoring of tree growth dynamics is essential to improve our understanding of the climatic controls that influence both tree-ring morphology and size. Timing of the ring formation can bring clues to improve interpretation of the tree-ring growth/climate models. In recent years, we set up monitoring networks to follow tree growth and obtain in situ weather data from forest ecosystems in Argentina and Mexico. At Cerro Krund, southern Tierra del Fuego, Argentina, a network of permanent plots was established along the altitudinal gradient of *Nothofagus pumilio*, from the valley bottom to the tree line. At a given plot, the initial surge of earlywood occurs after the first formed leaves are fully expanded; later, the cambium becomes most active and then finally ceases by producing latewood cells toward the end of summer. The influence of altitude is expressed in a delay of the onset of the initial growth stages (up to 2 weeks between lower and higher plots) and in the shortening of the vegetative growth period. At lower elevations the cambium remains active for 3–4 months, compared to only 2–3 months at the tree line. Rapid changes in temperature act as the environmental catalyst to force the changes of the leaf phenological phases and the wood morphological changes through the ring. Box Figure 7.17 shows a synchrony between a sustained increase of the maximum air temperatures to values above a threshold of 10°C and the beginning of the growth phases. Toward the end of austral summer, trees slowly end their growth cycle as maximum temperatures fall below this threshold line.

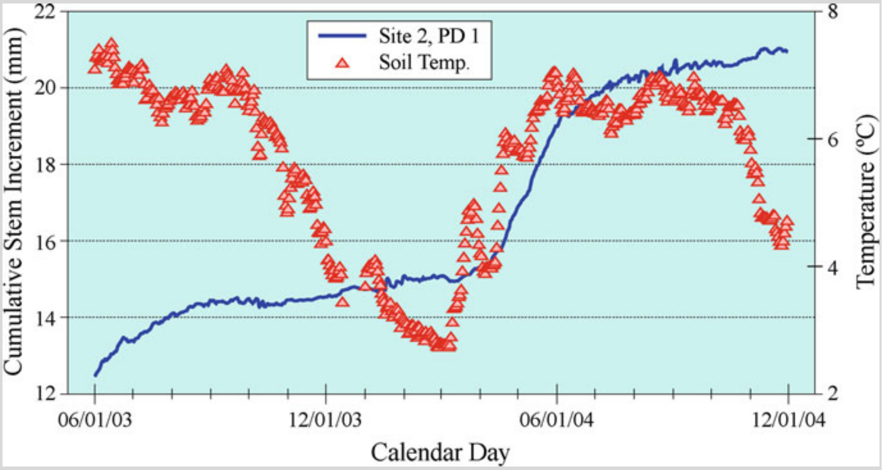

Box Fig. 7.18 Two seasons of growth are shown in the monitored *Pinus hartwegii* stand in southwestern Mexico. Onset of growth is coincident with the increase of spring temperatures above 3.6ºC. Continuation of growth is dependent on monsoon moisture

In Nevado de Colima, a 3900 m elevation site in central western México, we have been co-monitoring stem growth and weather on two plots of *Pinus hartwegii*. The monitoring network consists of a meteorological station and two sets of dendrometers installed on pure stands of *P. hartwegii* located ~100 m below tree line. This species has previously shown promise for paleoclimate analysis because of sensitivity to the North American Monsoon. Co-measuring tree growth and climate over a 3-year period has allowed a better understanding of the complex response of this species to changing environmental conditions. Box Figure 7.18 shows that the onset of spring growth is coincident with soil temperatures higher than a threshold of around 3.6ºC. Summer growth, however, is dependent on monsoon precipitation, with high correlations to precipitation and relative humidity. The pattern of growth mirrors the lull in the monsoon in late summer. We also have confirmed the cessation of growth and shutdown of cambial activity in the winter months at this high-elevation tropical site. Long-term ecological monitoring has allowed direct correlation at daily and monthly timescales between tree growth and weather. It is desirable that the monitoring previously described be continued over long time periods to better understand the radial growth behaviors.

—F. Roig, P. Hartsough, G Massacchesi, F. Biondi, and G. Martinez Pastur

In South America, the only chronologies that presently extend into the mid-Holocene are for *Fitzroya cupressoides* from southern Chile. The Volcan Apagado (41º35′S, 72º30′W) chronology is now the longest continuous chronology in the Southern Hemisphere, with a total of 5666 years (Wolodarsky-Franke et al. 2005). However, much more work is needed to develop multimillennial length chronologies encompassing most of the Holocene and employing other species in more arid regions of South America.

As in other areas of the world, it is also possible that anthropogenic activities may be subtly changing climate-growth relationships in these trees, compounding the difficulties of isolating a clear climate signal in these records. The recent high growth rates of *Nothofagus* at the upper tree line across Patagonia provide a major piece of evidence to assemble a case for anomalous regional warming in response to anthropogenic activities (Villalba et al. 2003). While this conclusion may prove to be a valid interpretation of the data, changes in the efficiency with which water is used in relation to increased atmospheric CO_2 content (fertilization), may also exert some influences on tree growth.

7.5 Discussion and Conclusions

Precisely dated, annually resolved tree-ring records from numerous sites throughout the Americas provide the basis to evaluate the changing signatures of tropical and high-latitude modes of climate variability, their time-evolving patterns, and their interactions in the past. Based on our present knowledge of climate variations during the twentieth century, we intended this contribution to provide an interhemispheric view of interactions between large-scale modes of variability and climate along the American Cordilleras over several centuries prior to the period of instrumental observations. The striking symmetries in SSTs across the equatorial Pacific and in sea level pressure (SLP) patterns at high latitudes in both hemispheres induce similar patterns of climate variability in widely separated regions of the western Americas (Dettinger et al. 2001).

Comparisons of fire histories between the southwestern United States and northern Patagonia over the past several centuries provide additional evidence for similarities in past climate variations across the extratropical Americas (Kitzberger et al. 2001). The synchrony of fire regimes in these two distant regions has tentatively been interpreted as a response to decadal-scale changes in ENSO and PDO activities. For example, a period of decreased fire occurrence in both regions from about 1780 to 1830 was attributed to decreased amplitude and/or frequency of ENSO events.

Strong interhemispheric symmetries of ENSO and ENSO-like variations of Pacific climate on decadal timescales produce similar patterns of temperature variations in Patagonia and the Gulf of Alaska. However, the comparison of these extratropical temperature reconstructions with the Raratonga temperature-sensitive coral record from the tropical Pacific indicates that over the last 200 years, interdecadal SST variations in the Pacific alternated between times of more geographically widespread interdecadal changes—such as the shift in the mid-1970s that was recorded across the entire Pacific basin—and times of less geographically organized interdecadal changes shared by the tropics and the north or south Pacific Ocean. Our observations that interdecadal variations in SST in the tropical Pacific were more strongly connected to the north Pacific in the twentieth century than in the mid-1800s agree with previous studies by Evans et al. (2001a) and Labeyrie et al. (2003).

In addition to tropical forcings, similarities in decadal- to century-scale climate variations also result from changes in high-latitude modes of climate variability that simultaneously affect the extratropical regions of North and South America. Instrumental records show a simultaneous intensification of the AO and AAO during recent decades (Thompson and Solomon 2002).

As was shown in Section 7.3.3, the annular modes are strongly coupled with surface air temperatures over high latitudes in both hemispheres (Thompson and Wallace 2000). Sustained positive trends in both modes in recent decades may be linked to large-scale warming, particularly in Eurasia and northern Canada in the Northern Hemisphere and across Patagonia in the Southern Hemisphere (Thompson and Wallace 2000; Thompson and Solomon 2002; Ogi et al. 2004). D'Arrigo et al. (2003) presented a first reconstruction of a warm season AO temperature index during the interval 1650–1975. Values during the middle twentieth century, overlapping with the anthropogenic increase in trace gases, equal or exceed those in the prior record. Lower values are reconstructed for several colder periods, including the early nineteenth-century interval. Trends in the AO temperature index resemble those of the tree-ring reconstructions of Arctic mean annual temperatures ($r = 0.47$, $n = 305$). According to D'Arrigo et al. (2003), the similarities between these records reflect some data overlap, but also the strong linkage between the AO and Arctic temperatures. Similarly, instrumental observations support a strong relationship between AAO and temperature in southern South America during the past 50 years, suggesting that long-term trends in temperature across Patagonia during the past centuries have also been influenced by changes in the AAO (Thompson and Solomon 2002).

As the reconstructions from high latitudes in both hemispheres indicate large similarities in temperature changes for at least the past 300 years, we could infer some common forcings of annular modes of climate variability in both hemispheres during the past centuries. Presumably, any climate change mechanism that projects onto the meridional temperature gradient between the middle and high latitudes may affect the polarity of the annular modes. Recent trends in tropical sea surface temperatures have been shown to affect the NAM (Hoerling et al. 2001), and it has been hypothesized (but not yet demonstrated) that a similar link may exist for the SAM (Hurrell and van Loon 1994).

Interactions between low- and high-latitude circulation modes are difficult to document based on the current array of climate-sensitive chronologies and forcing reconstructions. For example, interannual and decadal modes of tropical climatic variability such as ENSO and PDO strongly affect weather conditions in low latitudes of the western Americas, but their influences on the climate of the extratropics have been noted here and widely documented elsewhere. On the other hand, the annular modes have large amplitudes at extratropical latitudes, but several studies reveal that they have a substantial signature at lower latitudes as well (Thompson and Lorenz 2004).

Reflection symmetries about the equator in interdecadal ocean temperature during the past four centuries suggest that the tropical Pacific has played a pivotal role in linking westerly winds in both hemispheres through meridional teleconnections (Zhang et al. 1997; White and Cayan 1998). As has been indicated here, temperature-sensitive records from the Gulf of Alaska and northern Patagonian are coherent on long-term (>10 years) oscillatory modes, largely in response to ENSO-like decadal to interdecadal modes of variability in the Pacific Ocean. However, instrumental records show that high-latitude forcings of climate variability also affect both regions. For example, recent trends in Alaskan climate are better explained by the juxtaposition of ENSO-like and AO-related SLP variability over the north Pacific.

The 'ENSO-like' interdecadal variability, as documented in Trenberth and Hurrell (1994) and Zhang et al. (1997), has contributed to SLP declines over the north Pacific in conjunction with warming over western Canada and Alaska. Apart from that feature, SLP over the north Pacific has risen slightly during the past 30 year, consistent with the trend toward the 'high-index' state of the AO during this period. That the trend in the SAM accounts for approximately 50% of the warming over the Antarctic Peninsula and southern Patagonia attests to the importance of climate mechanisms other than ENSO over this region. In consequence, the additive effects of low- and high-latitude forcings on climates along the American Cordilleras hamper a current estimation of past interactions between tropical and high-latitude forcings. Independent reconstructions of tropical and polar modes of variability are needed to gain insight on past forcing interactions and the combined effect on climates of the western Americas.

Teleconnections between precipitation estimates and climatic forcings evolve over time, suggesting a changing global signature of ENSO and other forcings. Our results indicate that the timing of interdecadal transitions in temperature- and precipitation-sensitive records has not always been consistent across the region. In addition, the degree of correlation between records has varied over time. Over the last 400 years, interdecadal climate variations in the Pacific alternated between times of larger amplitude and more geographically widespread interdecadal changes and times of lower amplitude and less geographically organized interdecadal changes.

Most tree-ring records suggest that the interdecadal variability in the Pacific region was particularly more organized before the mid-1800s, whereas interannual variability increased after that period. These observations point to a major reorganization of the climate modes of variability in the Pacific around 1850, the generally accepted time of the end of a particularly cool period in the 1800s, identified in some regions as the end of the Little Ice Age (LIA; Grove 1988; Bradley and Jones 1992; Luckman and Villalba 2001).

Detailed analysis of the influences of tropical and high-latitude modes of climate variability across the American Cordilleras is somewhat constrained by the current length of the proxy records. Additional insight can be gained by extending the records to cover different climatic intervals, such as the 'warmer' medieval period. Jones et al. (2001), Mann and Jones (2003), and many other authors have stressed the critical need for developing longer proxy records of both regional climate variations and hemispheric climatic forcings. Longer proxy series can be used to evaluate the long-term natural behavior of these modes of variation and their regional impacts more comprehensively. In so doing, these extended series can provide a long-term context for variability during the period of increasing trace gases, and for testing climate prediction models. Proxy climate records stand as our only means of assessing the long-term variability associated with large-scale modes of climate variability and their global influences.

Acknowledgements We gratefully acknowledge the support of the Inter-American Institute for Global Change Research through its Collaborative Research Network Program for the past 6 years. Parts of this project have also been funded by a range of national, international, and nonprofit organizations.

References

Aceituno P (1988) On the functioning of the Southern Oscillation in the South American sector. Part I: surface climate. Mon Weather Rev 116:505–524

Aceituno P, Montecinos A (1996) Assessing upper limits of seasonal predictability of rainfall in central Chile based on SST in the equatorial Pacific. Exp Long-Lead Forecast Bull 5:37–40

Aravena JC, Lara A, Wolodarsky-Franke A, Villalba R, Cuq E (2002) Tree-ring growth patterns and temperature reconstruction from *Nothofagus pumilio* (Fagaceae) forests at the upper tree line of southern Chilean Patagonia. Rev Chil Hist Nat 75:361–376

Argollo J, Soliz C, Villalba R (2004) Potencialidad dendrocronológica de *Polylepis tarapacana* en los Andes Centrales de Bolivia. Ecología en Bolivia 39:5–24

Beamish RJ, Benson AJ, Sweeting RM, Neville CM (2004) Regimes and the history of the major fisheries off Canada's west coast. Prog Oceanogr 60:355–385

Boninsegna JA (1988) Santiago de Chile winter rainfall since 1220 as being reconstructed by tree rings. Quaternary South Am Antarctic Peninsula 4:67–87

Bradley RS, Jones PD (1992) When was the 'Little Ice Age'? In: Mikami T (ed) Proceedings of the international symposium on the Little Ice Age climate. Department of Geography, Tokyo Metropolitan University, Japan, pp 1–4

Brendel O, Iannetta PPM, Stewart D (2000) A rapid and simple method to isolate pure cellulose. Phytochem Anal 11:7–10

Chavez FP, Ryan J, Llucha-Cota SE, Niquen M (2003) From anchovies to sardines and back: multidecadal change in the Pacific Ocean. Science 299:217–221

Cleaveland MK (1986) Climatic response of densitometric properties in semiarid site tree rings. Tree-Ring Bull 46:13–29

Cleaveland MK, Stahle DW, Therrell MD, Villanueva-Diaz J, Burns BT (2003) Tree-ring reconstructed winter precipitation and tropical teleconnections in Durango, Mexico. Clim Change 59:369–388

Cobb KM, Charles CD, Cheng H, Edwards RL (2003) El Niño/Southern Oscillation and tropical Pacific climate during the last millennium. Nature 424:271–276

Cole JE, Cook ER (1998) The changing relationship between ENSO variability and moisture balance in the continental United States. Geophys Res Lett 25:4529–4532

Cook ER, Meko DM, Stahle DW, Cleaveland MK (1999) Drought reconstructions for the continental United States. J Clim 12:1145–1162

Cook ER, Cole JE, D'Arrigo RD, Stahle DM, Villalba R (2000) Tree-ring records of past ENSO variability and forcing. In: Diaz HF, Markgraf V (eds) El Niño and the Southern Oscillation: multiscale variability, global and regional impacts. Cambridge University Press, Cambridge, UK, pp 297–323

Cook ER, Woodhouse CA, Eakin CM, Meko DM, Stahle DW (2004) Long term aridity changes in the western United States. Science 306:1015–1018

D'Arrigo RD, Jacoby G (1993) Secular trends in high northern latitude temperature reconstructions based on tree rings. Clim Change 25:163–177

D'Arrigo RD, Villalba R, Wiles G (2001) Tree-ring estimates of Pacific decadal climate variability. Clim Dynam 18:219–224

D'Arrigo RD, Cook ER, Mann ME, Jacoby GC (2003) Tree-ring reconstructions of temperature and sea-level pressure variability associated with the warm-season Arctic Oscillation since AD 1650. Geophys Res Lett 30(11):1549. doi:10.1029/2003GL017250

D'Arrigo R, Wilson R, Deser C, Wiles G, Cook E, Villalba R, Tudhope S, Cole J, Linsley B (2005) Tropical-north Pacific climate linkages over the past four centuries. J Clim 18:5253–5265

Deser C, Blackmon M (1993) Surface climate variations over the North Atlantic Ocean during winter: 1900–1989. J Clim 6:1743–1753

Deser C, Wallace JM (1990) Large-scale atmospheric circulation features of warm and cold episodes in the tropical Pacific. J Clim 3:1254–1281

Deser S, Phillips A, Hurrell J (2004) Pacific interdecadal climate variability: linkages between the tropics and north Pacific during boreal winter since 1900. J Clim 17:3109–3124

Dettinger MD, Battisti DS, McCabe GJ, Bitz CM, Garreaud RD (2001) Interhemispheric effects of interannual and decadal ENSO-like climate variations on the Americas. In: Markgraf V (ed) Interhemispheric climate linkages. Academic, San Diego, pp 119–140

Ebbesmeyer CC, Cayan DR, McClain DR, Nichols FH, Peterson DH, Redmond KT (1991) 1976 step in the Pacific climate: forty environmental changes between 1968–75 and 1977–84. In:

Proceedings of the seventh annual Pacific climate (PACLIM) workshop. California Department of Water Resources, pp 115–126
Eischeid JK, Diaz HF, Bradley RS, Jones JD (1991) A comprehensive precipitation data set for global land areas. DOE/ER-69017T-H1, TR051, United States Department of Energy, Carbon Dioxide Research Program, Washington, DC
Enfield DB, Mestas-Nuñez AM (2000) Global modes of ENSO and non-ENSO sea surface temperature variability and their associations with climate. In: Diaz H, Markgraf V (eds) El Niño and the Southern Oscillation: multiscale variability and global and regional impacts. Cambridge University Press, Cambridge, UK, pp 89–112
Evans MN, Schrag DP (2004) A stable isotope-based approach to tropical dendroclimatology. Geochim Cosmochim Ac 68:3295–3305
Evans MN, Cane MA, Schrag DP, Kaplan A, Linsley BK, Villalba R, Wellington GM (2001a) Support for tropically-driven Pacific decadal variability based on paleoproxy evidence. Geophys Res Lett 28:3869–3692
Evans MN, Kaplan A, Cane MA, Villalba R (2001b) Globality and optimality in climate field reconstructions from proxy data. In: Markgraf V (ed) Interhemispheric climate linkages. Academic, San Diego, pp 53–72
Fritts H (1976) Tree rings and climate. Academic, London
Fritts H (1991) Reconstructing large-scale climatic patterns from tree-ring data. University of Arizona Press, Tucson
Garreaud R, Battisti DS (1999) Interannual and interdecadal (ENSO-like) variability in the Southern Hemisphere tropospheric circulation. J Clim 12:2113–2123
Garreaud R, Vuille M, Clement A (2003) The climate of the Altiplano: observed current conditions and mechanisms of past changes. Palaeogeogr Palaeocl 194:5–22
Gershunov A, Barnett TP (1998) Interdecadal modulation of ENSO teleconnections. B Am Meteorol Soc 79:2715–2725
Gong D, Wang S (1999). Definition of Antarctic Oscillation index. Geophys Res Lett 26:459–462
Graham NE (1994) Decadal-scale climate variability in the 1970s and 1980s: observations and model results. Clim Dynam 10:135–162
Graham NE, Hughes MK, Ammann CM, Cobb KM, Hoerling MP, Xu T, Kennett DJ, Kennett JP, Rein B, Stott L, Wigand PE (2007) Tropical Pacific-mid-latitude teleconnections in Medieval times. Clim Change 83:241–285
Grove JM (1988) The Little Ice Age. Methuen, London, 498 pp
Hartsough P, Biondi F (2003) The importance of high elevation monitoring in a tropical treeline environment: a project update from southwestern Mexico. In: Fourth annual science meeting, IAI CRN03, Abstracts, p 18
Hoerling MP, Hurrell JW, Xu T (2001) Tropical origins for recent North Atlantic climate change. Science 292:90–92
Hughes MK, Funkhouser G (1998) Extremes of moisture availability reconstructed from tree rings for recent millennia in the Great Basin of western North America. In: Beniston M, Innes JL (eds) The impacts of climate variability on forests. Springer, Berlin, pp 99–107
Hurrell JW, van Loon H (1994) A modulation of the atmospheric annual cycle in the Southern Hemisphere. Tellus 46A:325–338
Hurrell JW, van Loon H (1997) Decadal variations associated with the North Atlantic Oscillation. Clim Change 36:301–326
Jones PD, Moberg A (2003) Hemispheric and large-scale surface air temperature variations: an extensive revision and update to 2001. J Clim 16:206–223
Jones PD, Raper SCB, Bradley RS, Diaz HF, Kelly PM, Wigley TML (1986a) Northern Hemisphere surface air temperature variations: 1851–1984. J Clim Appl Meteorol 25:161–179
Jones PD, Raper SCB, Wigley TML (1986b) Southern Hemisphere surface air temperature variations: 1851–1984. J Clim Appl Meteorol 25:1213–1230
Jones PD, Osborn TJ, Briffa KR (2001) The evolution of climate over the last millennium. Science 292:662–667

Karoly DJ (1990) The role of transient eddies in low-frequency zonal variations of the Southern Hemisphere circulation. Tellus 42A:41–50

Kennett DJ, Kennett JP (2000) Competitive and cooperative responses to climatic instability in coastal southern California. Am Antiquity 65(2):379–395

Kessler M (1995) The genus Polylepis (Rosaceae) in Bolivia. Candollea 50:1–172

Kiladis GN, Diaz HF (1989) Global climatic anomalies associated with extremes of the Southern Oscillation. J Clim 2:1069–1090

Kitzberger T, Swetnam TW, Veblen TT (2001) Inter-hemispheric synchrony of forest fires and the El Niño-Southern Oscillation. Global Ecol Biogeogr 10:315–326

Labeyrie L, Cole J, Alverson K, Stocker T (2003) The history of climate dynamics in the late quaternary. In: Alverson KD, Bradley RS, Pedersen TF (eds) Paleoclimate, global change and the future. IGBP Series, Springer, Berlin, pp 33–62

LaMarche VC (1975) Potential of tree rings for reconstruction of past climate variations in the Southern Hemisphere. In: Proceedings of the WMO/IAMAP symposium on long term climatic fluctuations, Norwich, England. World Meteorological Organization, WMO No. 421, Geneva, pp 21–30

Lara A, Aravena JC, Villalba R, Wolodarsky-Franke A, Luckman B, Wilson R (2001) Dendroclimatology of high-elevation *Nothofagus pumilio* forests at their northern distribution limit in the central Andes of Chile. Can J Forest Res 31:925–936

Lara A, Villalba R, Wolodarsky-Franke A, Aravena JC, Luckman BH, Cuq E (2005) Spatial and temporal variation in *Nothofagus pumilio* growth at treeline along its latitudinal range (35º40′ to 55ºS) in the Chilean Andes. J Biogeogr 32:879–893

Lenters JD, Cook K (1999) Summer-time precipitation variability over South America: role of the large scale circulation. Mon Weather Rev 127:409–431

LeQuesne C, Stahle DW, Cleaveland MK, Therrell MD, Aravena JC, Barichivich J (2006) Ancient ciprés tree-ring chronologies used to reconstruct central Chile precipitation variability from AD 1200–2000. J Clim 19:5731–5744

Linsley B, Wellington G, Schrag D, Ren L, Salinger M, Tudhope A (2004) Geochemical evidence from corals for changes in the amplitude and spatial pattern of South Pacific interdecadal climate variability over the last 300 years. Clim Dynam 22:1–11

Luckman BH, Boninsegna JA (2001) The assessment of present, past and future climate variability in the Americas from treeline environments. PAGES Newsletter 9:17–19

Luckman BH, Villalba R (2001) Assessing the synchroneity of glacier fluctuations in the Western Cordillera of the Americas during the last millennium. In: Markgraf V (ed) Interhemispheric climate linkages. Academic, San Diego, pp 119–140

Luckman BH, Wilson RJS (2005) Summer temperature in the Canadian Rockies during the last millennium: a revised record. Clim Dynam 24:131–144

Luckman BH, Briffa KR, Jones PD, Schweingruber FH (1997) Summer temperatures at the Columbia Icefield, Alberta, Canada, 1073–1983. Holocene 7:375–389

Mann ME, Jones PD (2003) Global surface temperatures over the past two millennia. Geophys Res Lett 30, art 1820

Mann ME, Bradley RS, Hughes MK (2000) Long-term variability in El Niño/Southern Oscillation and associated teleconnections. In: Diaz HF, Markgraf V (eds) El Niño and the Southern Oscillation: multiscale variability, global and regional impacts. Cambridge University Press, Cambridge, UK, pp 357–412

Mantua JN, Hare SR (2002) The Pacific Decadal Oscillation. J Oceanogr (Japan) 58:35–44

Mantua JN, Hare SR, Zhang Y, Wallace JM, Francis RC (1997) A Pacific interdecadal climate oscillation with impacts on salmon production. B Am Meteorol Soc 78:1069–1080

Martínez M (1963) Las pináceas mexicanas, 3rd edn. Instituto de Biología, Universidad Nacional Autónoma de México, México

Meko D, Cook ER, Stahle DW, Stockton CW, Hughes MK (1993) Spatial patterns of tree-growth anomalies in the United States and southeastern Canada. J Clim 6:1773–1786

Montecinos A, Aceituno P (2003) Seasonality of the ENSO-related rainfall variability in central Chile and associated circulation anomalies. J Clim 16:281–296

Ogi M, Yamazaki K, Tachibana Y (2004) The summertime annular mode in the Northern Hemisphere and its linkage to the winter mode. J Geophys Res 109:D20114. doi:10.1029/2004JD004514

Quinn WH, Neal VT (1983) Long-term variations in the Southern Oscillation, El Niño, and the Chilean subtropical rainfall. Fish B 81:363–374

Rein B, Lueckge A, Sirocko F (2004) A major Holocene ENSO anomaly in the medieval period. Geophys Res Lett 31, L17211. doi:10.1029/2004GL020161

Rein B, Lueckge A, Reinhardt L, Sirocko F, Wolf A, Dullo W-C (2005) El Niño variability off Peru during the last 20,000 years. Paleoceanography 20. doi:10.1029/2004PA001099

Roden JS, Lin G, Ehleringer JR (2000) A mechanistic model for interpretation of hydrogen and oxygen ratios in tree-ring cellulose. Geochim Cosmochim Ac 64:21–35

Rodriguez R, Mabres A, Luckman B, Evans M, Masiokas M, Ektvedt T (2005) 'El Niño' events recorded in dry-forest species of the lowlands of northwest Peru. Dendrochronologia 22:181–187

Roig FA, Martínez Pastur G, Massaccesi G, Pinedo L (2003) Toward an interpretation of the interactions between cambial activity, phenology and climate in *Nothofagus pumilio* forests of Tierra del Fuego, Argentina. In: Fourth annual science meeting, IAI CRN 03, Abstracts, pp 33–34

Ropelewski CF, Halpert MS (1986) North American precipitation and temperature patterns associated with El Niño/Southern Oscillation (ENSO). Mon Weather Rev 115: 1606–1626

Rutlland J, Fuenzalida H (1991) Synoptic aspects of the central Chile rainfall variability associated with the Southern Oscillation. Int J Climatol 11:63–76

Stahle DW, D'Arrigo RD, Krusic PJ, Cleaveland MK, Cook ER, Allan RJ, Cole JE, Dunbar RB, Therrell MD, Gay DA, Moore MD, Stokes MA, Burns BT, Villanueva-Diaz J, Thompson LG (1998) Experimental dendroclimatic reconstruction of the Southern Oscillation. B Am Meteorol Soc 79(10):2137–2152

Stine S (1994) Extreme and persistent drought in California and Patagonia during mediaeval time. Nature 369:546–549

Stott LD, Cannariato KG, Thunell R, Haug GH, Koutavas A, Lund S (2004) Decline of surface temperature and salinity in the western tropical Pacific Ocean in the Holocene epoch. Nature 431:56–59

Thompson DWJ, Lorenz DJ (2004) The signature of the annular modes in the tropical troposphere. J Clim 17:4330–4342

Thompson DWJ, Solomon S (2002) Interpretation of recent Southern Hemisphere climate change. Science 296:895–899

Thompson DWJ, Wallace JM (2000) Annular modes in the extratropical circulation. Part I: Month-to-month variability. J Clim 13:1000–1016

Trenberth K, Hurrell J (1994) Decadal atmospheric-ocean variations in the Pacific. Clim Dynam 9:303–19

Vautard R (1995) Patterns in time: SSA and MSSA. In: von Storch H, Navarra A (eds) Analysis of climate variability, applications of statistical techniques. Springer, Berlin, pp 259–279

Vautard R, Ghil M (1989) Singular spectrum analysis in nonlinear dynamics, with applications to paleoclimatic time series. Physica D35:395–424

Villalba R, Boninsegna JA, Veblen TT, Schmelter A, Rubulis S (1997) Recent trends in tree-ring records from high elevation sites in the Andes of northern Patagonia. Clim Change 36:425–454

Villalba R, D'Arrigo RD, Cook ER, Wiles G, Jacoby GC (2001) Decadal-scale climatic variability along the extratropical western coast of the Americas: evidences from tree-ring records. In: Markgraf V (ed) Interhemispheric climate linkages. Academic, San Diego, pp 155–172

Villalba R, Lara A, Boninsegna JA, Masiokas M, Delgado S, Aravena JC, Roig FA, Schmelter A, Wolodarsky A, Ripalta A (2003) Large-scale temperature changes across the southern Andes: twentieth-century variations in the context of the past 400 years. Clim Change 59: 177–232

Vuille M (1999) Atmospheric circulation over the Bolivian Altiplano during dry and wet periods and extreme phases of the Southern Oscillation. Int J Climatol 19:1579–1600

Vuille M, Bradley RS, Keimig F (2000) Interannual climate variability in the central Andes and its relation to tropical Pacific and Atlantic forcing. J Geophys Res 105:12447–12460

Wallace JM, Rasmusson EM, Mitchell TP, Kousky VE, Sarachik ES, von Storch H (1998). On the structure and evolution of ENSO-related climate variability in the tropical Pacific: lessons from TOGA. J Geophys Res 103:12241–14259

Watson E, Luckman BH (2004a) Tree-ring based reconstructions of precipitation for the southern Canadian Cordillera. Clim Change 65:209–241

Watson E, Luckman BH (2004b) Tree-ring estimates of mass balance at Peyto Glacier for the last three centuries. Quaternary Res 62:9–18

Watson E, Luckman BH (2005) Spatial patterns of pre-instrumental moisture variability in the southern Canadian Cordillera. J Clim 18:2847–2863

White W, Cayan DR (1998) Quasi-periodicity and global symmetries in interdecadal upper ocean temperature variability. J Geophys Res 103:21335–21354

Wiles GC (1997) North Pacific atmosphere-ocean variability over the past millennium inferred from coastal glaciers and tree rings. In: Preprint volume, Eighth symposium on global change studies. American Meteorological Society, 2–7 February 1997, Long Beach, California. pp 218–220

Wiles GC, Calkin PE (1994) Late Holocene, high-resolution glacial chronologies and climate, Kenai Mountains, Alaska. Geol Soc Am Bull 106:281–303

Wiles GC, D'Arrigo RD, Jacoby GC (1996) Temperature changes along the Gulf of Alaska and the Pacific Northwest coast modeled from coastal tree rings. Can J Forest Res 26:474–481

Wiles GC, D'Arrigo RD, Jacoby GC (1998) Gulf of Alaska atmosphere-ocean variability over recent centuries inferred from coastal tree-ring records. Clim Change 38:289–306

Wiles GC, D'Arrigo RD, Villalba R, Calkin PE, Barclay DJ (2004) Century-scale solar variability and Alaskan temperature change over the past millennium. Geophys Res Lett 31:L15203. doi:1029/2004GL020050

Wolodarsky-Franke A, Moreno P, Lara A, Pino M, Villarosa G (2005) Tree-ring, stratigraphic, and palynological evidence for volcanic and climatic controls on *Fitzroya cupressoides* forests in southern Chile, over the last 5700 years. In: Piovano EL, Leroy S (eds) Holocene environmental catastrophes in South America: from the lowlands to the Andes. Abstract volume and field guide. 11–17 Third joint meeting of the International Council for Science, Dark Nature and the International Geological Correlation Programme 490, March 2005, Miramar-Córdoba

Zhang Y, Wallace JM, Battisti DS (1997) ENSO-like interdecadal variability: 1900–93. J Clim 10:1004–1020

Zielinski GA (2000) Use of paleo-records in determining variability within the volcanism-climate systems. Quaternary Sci Rev 19:417–438